ISSN 0429-8284

Whole Number 176

FUJI ELECTRIC REVIEW

1

1997 VOL.43

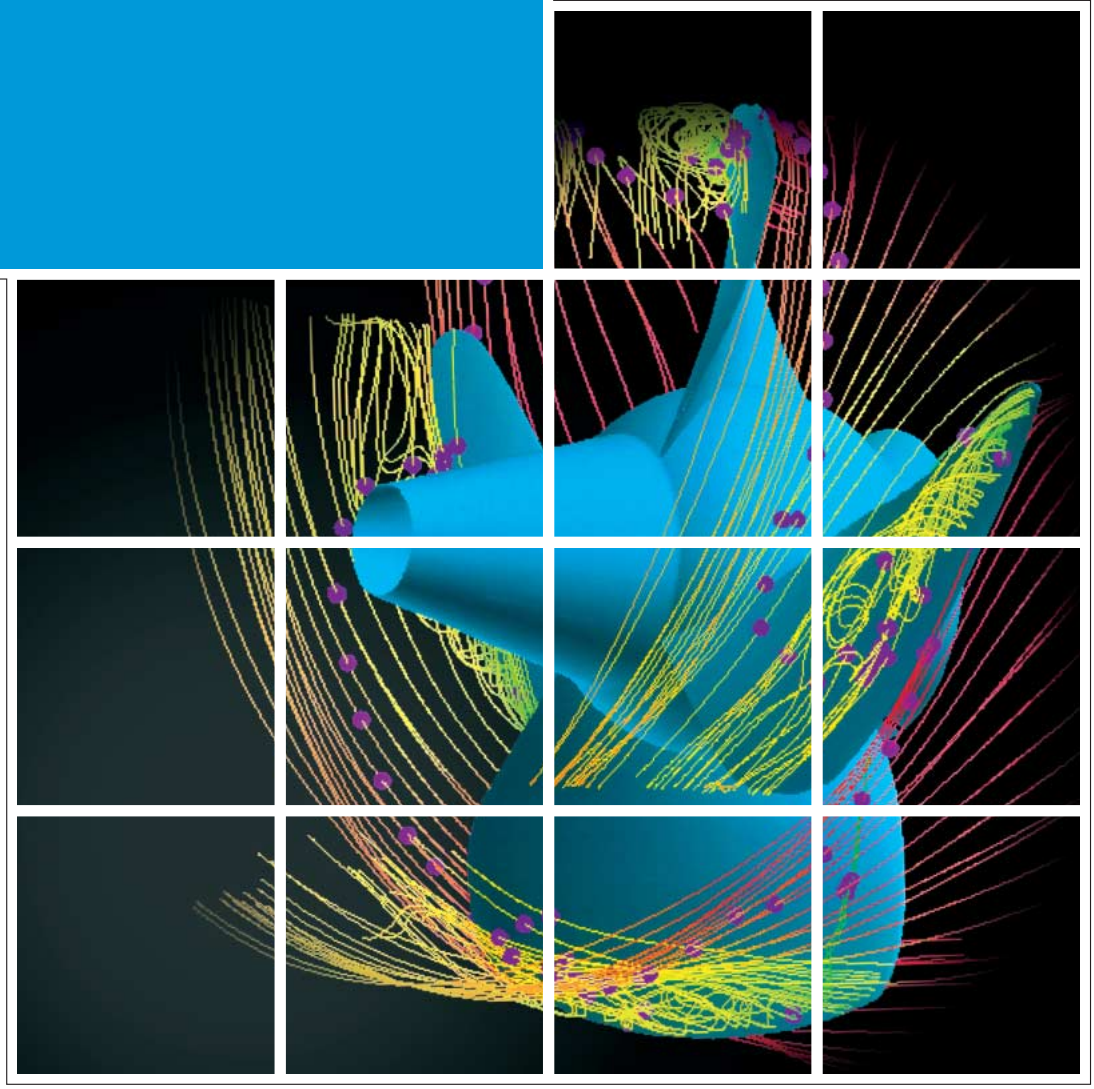

FUJI ELECTRIC

Creating a Better Tomorrow with Trustworthy Technology

Great Potential in the Coming Age, —
Fuji Electric's Hydropower Equipment

Fuji Electric has provided any kind of turbines and generators in the field of hydropower plant. Also the company can meet all needs from distribution systems to automated, total management and control systems through integrated system design.

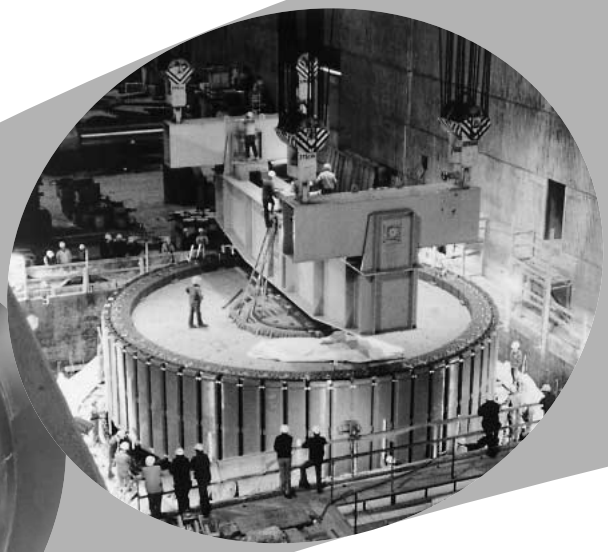

500MW Francis turbine-generator

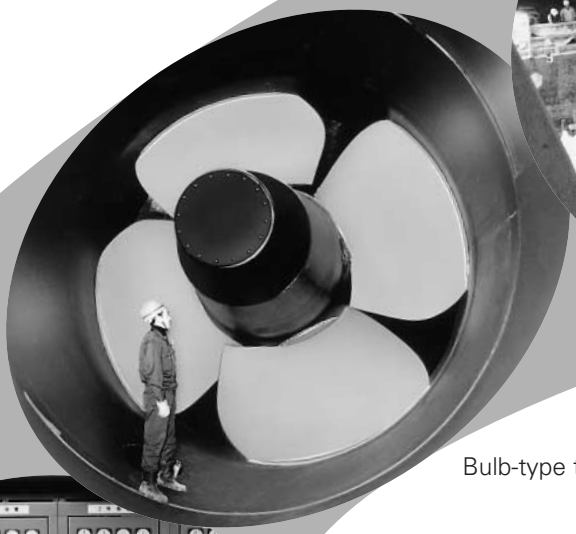

Bulb-type turbine

Hydropower plant simulator

Pelton-type turbine

200MW pumped storage power plant

FUJI ELECTRIC
REVIEW

1
1997 VOL.43

CONTENTS

Cover Photo:

With the rapid development of computer technology, particularly the price reduction and speed increase of workstations and personal computers, the serviceability of simulation technology is increasing in many fields.

Fuji Electric early developed its own simulation software and has utilized it for developing and designing various products.

The cover photo is an analysis example of leakage flow around the runner of a bulb turbine, displaying vortex formation over the low pressure side of the blade surface using the three-dimensional viscous-flow analysis software developed by Fuji Electric.

Fuji Electric Co.,Ltd. Head Office : No.12-1, 1-chome, Yurakucho, Chiyoda-ku, Tokyo, Japan

Bulb Turbine/Generator for Minokawai Power Plant, The Kansai Electric Power Co., Inc.

Hiroshi Ohta
Masataka Sunaga
Takanori Namiki

1. Introduction

Recently in the field of hydro energy development both in Japan and overseas, the benefits of using bulb turbine/generators at low head construction sites where the head is 25m or less have been reconsidered as a means to effectively develop domestic energy sources. And in response, the planning & development of power plants equipped with bulb turbine/generators is underway.

Fuji Electric has manufactured and delivered numerous large size and large capacity bulb turbine/generators ever since delivering the first large capacity bulb turbine/generator in Japan to the Akao Power Plant of The Kansai Electric Power Co., Inc. in 1978.

The Kansai Electric Power's Minokawai Power Plant (Figs. 1 & 2) was recently put into its commercial operation following an inspection by the Ministry of Trade and begun Commerce. Fuji Electric delivered a bulb turbine unit with a runner diameter of 5.55m, a bulb generator with a stator frame external diameter of 7.0m, and a control system etc. to the Minokawai Power Plant.

Table 1 shows the recent manufacturing history of large bulb turbine/generators.

As shown in Table 1, the turbine/generator for the Minokawai Power Plant ranks among the top group for both runner diameter and power output. In addition, it is also an advanced bulb turbine/generator that utilizes numerous new technologies in design, manufacture and installation. A summary of the new technology is introduced in the following report.

2. Project Summary

This project is located on the right bank of the Imawatari Dam, situated approximately 800m downstream of the point where the Kiso River and the Hida River merge, this project utilizes the abundant water flow discharged from the Imawatari Dam. This dam type power plant provides a maximum power generation of 23,400kW, has a maximum water consumption of 220m^3/s and an effective head of 12.36m.

As shown in Fig. 1, this is an urban type power plant where the powerhouse is located in close proximity to the consumers, which is rather rare for a hydropower plant.

Figures 3 and 4 illustrate, cross sections of the overall power plant and the turbine/generator, respectively.

Equipment specifications are listed below.

(1) Turbine
Max. power output : 24,200 kW
Effective head : 12.36/12.16m
Water consumption : 220 m^3/s
Rated speed : 100 r/min

Fig.1 Vicinity of power plant

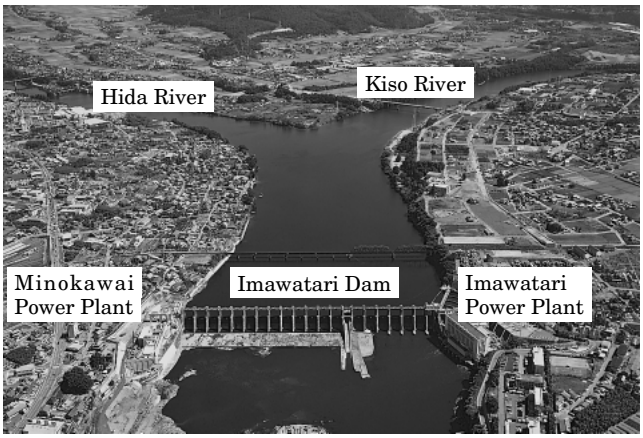

Fig.2 External view of power plant after its completion

Table 1 History of Fuji large bulb turbine/generators

Item / Power plant	No. of units	Turbine output (kW)	Head (m)	Speed (r/min)	Runner diameter (mm)	Generator output (kVA)	Voltage (kV)	Frequency (Hz)	Commercial operation
Akao, The Kansai Electric Power Co., Inc.	1	34,000	17.40	128.6	5,100	36,000	6.6	60	Oct. 1978
Sakuma #2, Power Development Co., Ltd.	2	16,800/ 16,000	15.50	125.0 150.0	4,485	17,000	6.6	50/60	Jul. 1982
Shingo #2, Tohoku Electric Power Co., Inc.	1	40,600	22.45	136.0	5,000	40,900	6.6	50	Sept. 1984
Main Canal Headworks, U.S.A.	1	26,800	12.80	112.5	5,350	27,370	6.9	60	Jul. 1986
Lower Mettur, India	8	17,200	7.53	75.0	6,250	18,333	6.6	50	Nov. 1987
New Martinsville, U.S.A.	2	20,040	6.40	64.0	7,300	21,620	6.6	60	Aug. 1988
Yamazato #2, Tohoku Electric Power Co., Inc.	1	23,700	15.93	125.0	4,750	24,100	6.6	50	Jun. 1992
Bailongtan, China	6	33,000	9.70	93.8	6,400	33,684	10.5	50	Under construction
Chashma, Pakistan	8	23,700	13.80	85.7	6,300	26,000	11.0	50	Being designed
Minokawai, The Kansai Electric Power Co., Inc.	1	24,200	12.16	100.0	5,550	26,000	6.6	60	May 1995

Fig.3 Cross section of power plant

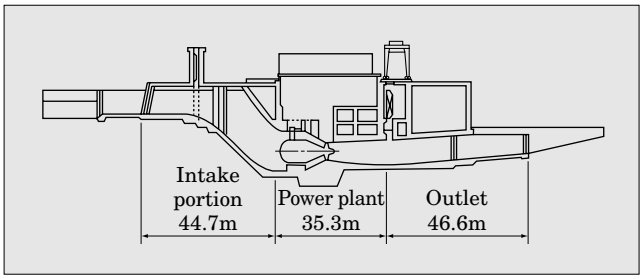

Fig.4 Cross section of turbine/generator

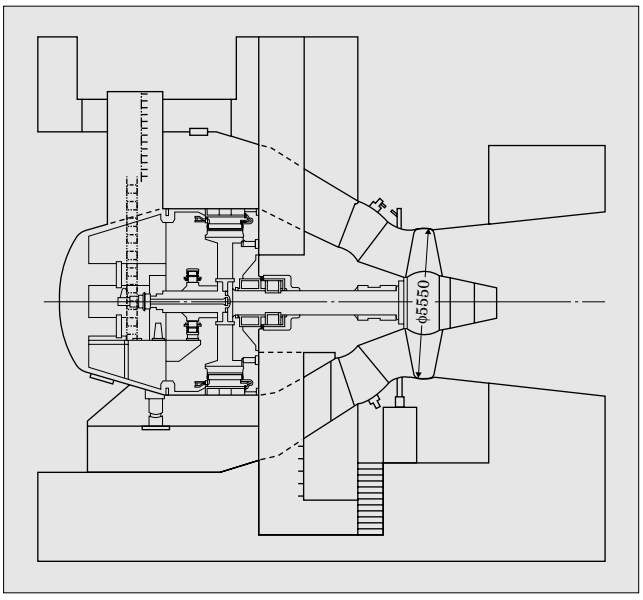

Specific speed : 685 m-kW
Runner diameter : 5,550 mm
Max. hydraulic pressure : 30 m
Max. speed rise : 70%

(2) Generator
Type : Vertical shaft, revolving magnetic field, water-water heat exchanger, 3-phase synchronous generator (Fin cooling)
Max. power output : 26,000 kVA
Rated voltage : 6.6 kV
Rated current : 2,274 A
Rated frequency : 60 Hz
Rated speed : 100 r/min
Rated power factor : 0.9 (lag)
Stator frame outer diameter : 7,000 mm
Excitation method : Brushless excitation

3. Characteristics

3.1 Bulb support method

Since the bulb which houses the turbine and generator is placed in a water passage, in addition to static loads such as hydraulic thrust force, dead weight, buoyancy, generator torque, etc., it receives mechanical vibrations from the rotating part and hydraulic vibrations due to hydraulic pressure fluctuation. Therefore, for this project, a method to support the bulb with two vertical (upper & lower) stay vanes and an auxiliary supporting method, the anti-vibration stay and casing support, are provided as illustrated in Fig. 5 in an effort to increase the bulb's natural vibration frequency.

The upper stay vane is used as the passage for inspecting turbine bearings, shaft seals etc. The lower stay vane, which also provides access to the turbine chamber, houses the oil and water drain pipes.

Also, a ladder had been provided in conventional stay vanes to enter and exit the turbine chamber. However in this project a spiral staircase was installed for reasons of safety and convenience and to improve

Fig.5 Construction of bulb support

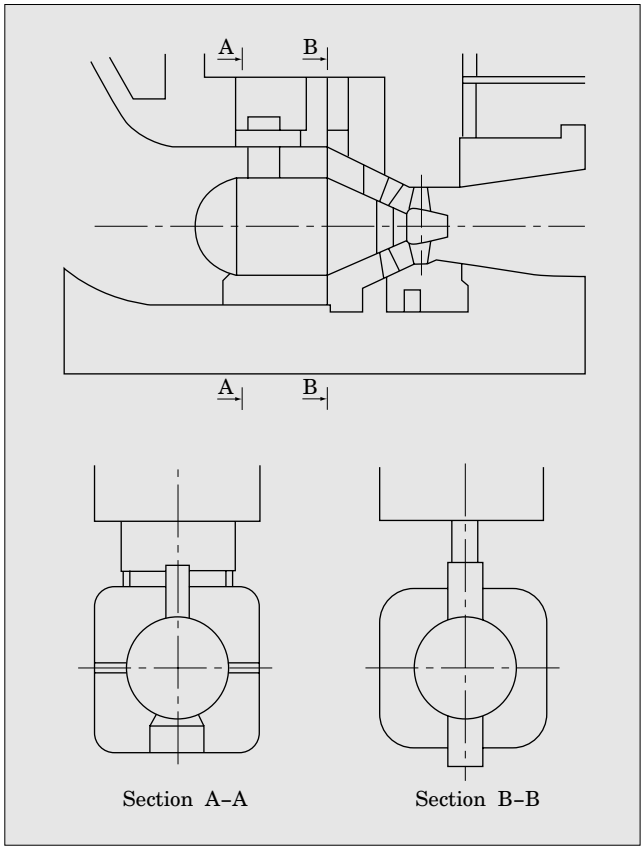

Fig.6 Complete turbine runner

N89-6388-108

its maintainability.

3.2 Turbine runner

The 4 blades of the turbine runner consist of 13% chrome and 4% nickel stainless cast steel, and are made movable so as to increase the partial load efficiency. The servomotor, which operates the runner vane, is housed in the runner boss, and the pressurized oil for operating the runner vane is supplied through the pressure oil distributing head located at the end of the generator shaft.

Fig.7 Ceramic seal system

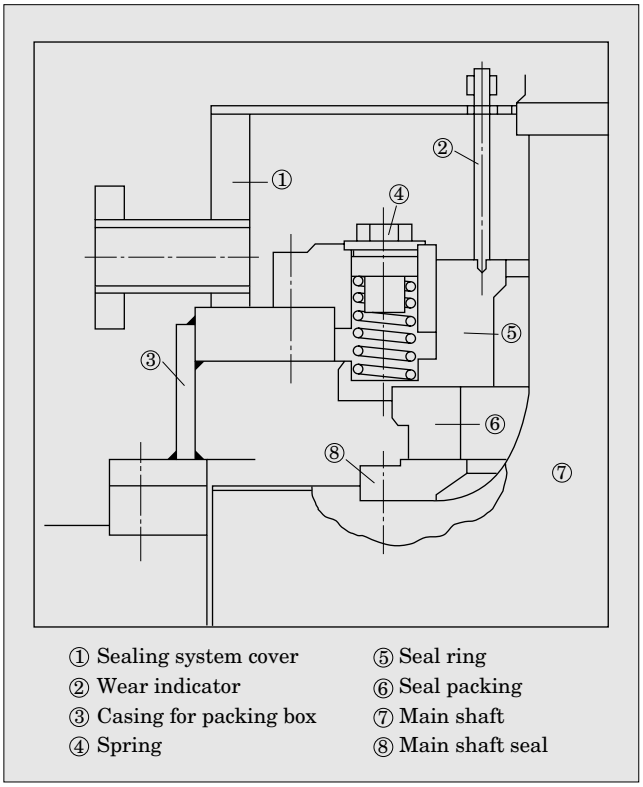

Fig.8 Closed circulation method with water-water cooler

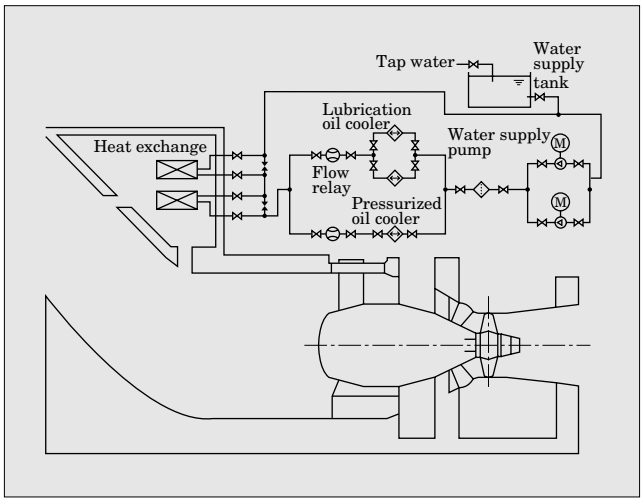

Normally, parts inside the runner boss such as the link are lubricated by oil. For this project however, it was decided to use water instead of oil for lubrication, since the construction site of this project is located at the bottom of the Kiso River and the prevention of river pollution was a major concern.

This bulb turbine was the first in the world to have a servomotor housed inside a water-filled boss runner. Methods to defect leakage, of servomotor oil in the runner boss for example, were given special consideration.

Figure 6 shows a photograph of the completed runner.

3.3 Main shaft sealing system

A ceramic seal system was used to seal the main shaft. This ceramic seal system is a mechanical seal that has ceramic overlays on the seat side of the main shaft and uses resin packing for the seal packing. The application of this system has benefits such as a simpler water supply system and improved friction/wear characteristics, compared to the conventional sealing system which uses the carbon packing method.

Figure 7 shows the construction of the ceramic sealing system.

3.4 Water supply system

A closed-circulation method with a water-water cooler was adapted for the water supply system for the pressurized oil and the lubrication oil. The closed-circulation method is, as illustrated in Fig. 8, a method to exchange the heat of cooling water (circulation water) at the pressurized oil and lubrication oil cooler, using a water-water cooler located at the top of the powerhouse water intake. The cooling water is forcefully circulated by pump.

To determine the location to install the water-water cooler, hydraulic model tests were conducted at the Technical Research Laboratory of The Kansai Electric Power Co., Inc., in order to confirm that the specified flow velocity could be obtained.

With the application of this method, the water supply system will be simplified. For example, compared to the conventional direct water supply system (a method of direct intake and use of river water as cooling water), the strainer is eliminated. In addition, the use of clear water (tap water) for the closed-circulation water has contributed to improved reliability of the water supply system, which is often problematic at hydropower generating facilities.

Fig. 9 Generator fan cooling method

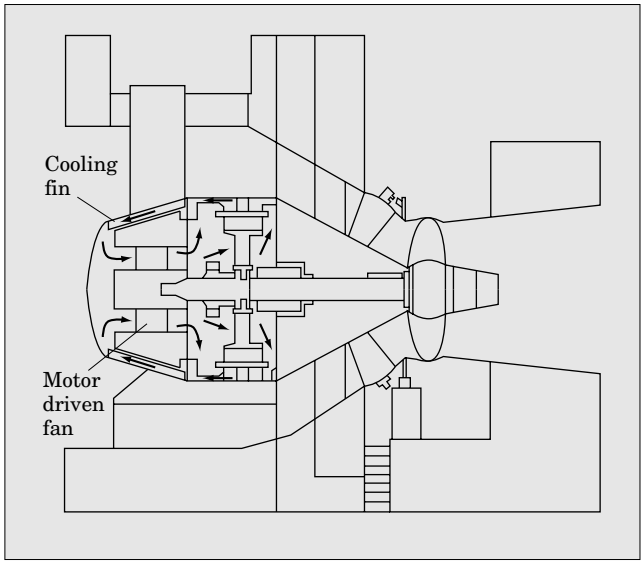

Fig. 10 Construction of bulb's internal monitoring system

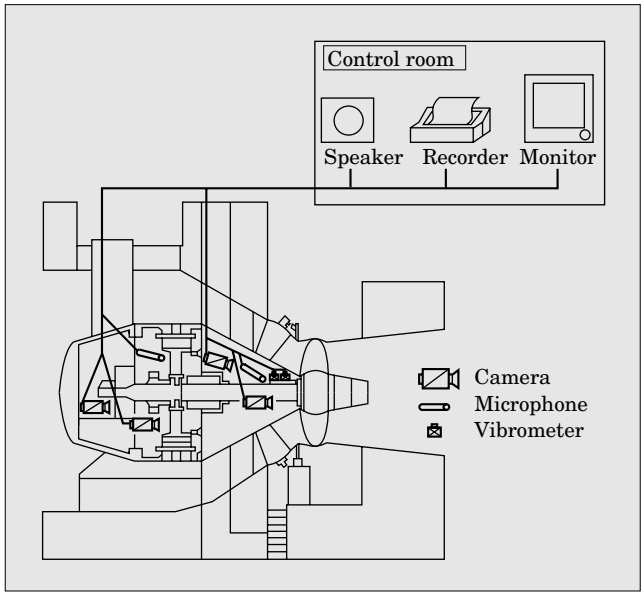

Table 2 History of fin-cooled bulb turbine/generator

Item / Power plant	No. of units	Generator output (kVA)	Voltage (kV)	Speed (r/min)	Temperature of cooling air at rib outlet (°C)	Remarks
Minokawai, The Kansai Electric Power Co., Inc.	1	26,000	6.6	100	50	
Sakuma #2, Power Development Co., Ltd.	2	17,000	6.6	125 150	50	Pressure rise 1.0 atmospheric pressure
Merced Main Canal, U.S.A.	1	2,830	4.16	180	45	
Dawson, U.S.A.	1	4,660	4.16	120	50	
Itado, Akita Prefecture	1	2,040kW	6.6	375	60	Induction generator
Yuda, Kyushu Electric Power Co., Inc.	1	5,750	6.6	150	50	
Oya, Fukushima Prefecture	1	3,470	6.6	214	52	
Nibudani, Hokkai Hydropower Generation	1	3,060	6.6	250	50	

3.5 Generator cooling method

Fin cooling was used to cool the generator. As illustrated in Fig. 9, the fin cooling method is a method in which steel cooling fins, attached to the stator frame and inner wall of the top nose of the bulb, are cooled by river water that flows around the outside of the bulb and cooled air is circulated inside the bulb with a motor-driven fan. The application of this method made it possible to eliminate conventional air coolers, resulting in easier maintenance.

Further, in the conventional air cooler, the area of the outer casing to be cooled needs to be increased as the generator capacity increases, thereby limiting the applicable power output. However, by changing the coating of the bulb's outer wall (river water side) from conventional corrosion resistant paint to an aluminum metallic coating, in order to reduce heat resistance of the heat radiating area, fin cooling could be applied on a larger scale in this project.

Although this fin cooling method has been applied to medium/small bulb generators, prior to this project it had not been used in large capacity bulb generators. To date, this project is the largest capacity bulb generator in the world that uses the fin cooling method.

Table 2 shows the history of the fin-cooled bulb turbine/generator.

3.6 Control system

A total digital control system equipped with a programmable controller is used to control the turbine/generators. With this total digital control system, the main unit sequence control function, governor function, automatic voltage control function and automatic synchronization control function are controlled by a single programmable controller unit. Previously, separate control systems had been utilized, however the realization of a programmable controller having high speed arithmetic operation made it possible to control all functions and thus to eliminate the control board.

3.7 Status monitoring system

A monitoring system in the control room was introduced, in which movable and fixed type ITV systems and microphones are installed in the turbine and generator chambers in order to externally monitor equipment status and to improve equipment maintainability.

Additional systems, such as a thermometer/hygrometer, vibrometer, oxygen densitometer etc., are provided to constantly monitor conditions inside the bulb.

Figure 10 illustrates the construction of the bulb's internal monitoring system.

3.8 Site installation procedure

In this project, outdoor gantry cranes were used to install the equipment. Although use of outdoor gantry cranes for the installation of equipment may risk prolonging the work schedule due to inclement weather, this project was able to achieve a considerably short installation period compared to the usual installation period for a bulb turbine, due to thorough preliminary preparation for rainy weather, an efficient use of the site assembly floor, and the application of new techniques to the turbine installation.

Explanations of the new techniques for turbine installation are given below.

To install the inner/outer casings and guide vane rings in a turbine, normally the inner/outer casings are assembled and installed, concrete is allowed to set, and then the strain on the surface of the downstream side casing flange is corrected. Next the inner/outer guide vane rings are assembled and installed. However for this project, the inner/outer casings and inner/outer guide vane rings of the turbine are simultaneously assembled and installed, followed by the application of concrete. As a result, the time necessary to correct strain on the downstream side flange surface was eliminated, shortening the construction period by more than 14 days.

This was the first time for Fuji Electric to use this technique, and a successful application of this technique requires continuous monitoring, during application of the concrete, of the strain on casings and guide vane rings, the concrete temperature etc. from the start to the completion of the concrete work. For this project, the inner/outer casings and guide vane rings were safely installed without any indications of harmful strain due largely to the cooperation from relevant individuals such as the civil contractor.

4. Conclusion

The characteristics and summary of the bulb turbine/generator for the Minokawai Power Plant were described in this report.

The authors assume there will be increased demand in the future for developing and planning power plants equipped with large size and capacity bulb turbines, and would be grateful if this report will become of reference, to whatever degree, for future development/planning works.

26MW Pelton Turbine for Nikengoya Power Plant, Chubu Electric Power Co., Inc.

Masamichi Makino
Hiromu Hayama
Takashi Tozaki

1. Introduction

Making hydropower plants more economical is the most important subject in promoting their development. Particularly in recent Japan, most of the large and economical hydropower resources have already been developed, leaving the remaining hydropower resources limited to either ultra low head or high head resources. Of the various turbines, Pelton turbines, which are used at high head resources, are often installed in secluded mountainous areas. Such hydropower resources are becoming more remote every year. Therefore the construction and maintenance costs tend to be higher compared to those of existing hydropower resources.

Under these circumstances, the Nikengoya Power Plant with a 6-jet Pelton turbine began its commercial operation in June of 1995. The main turbine/generator specifications for this power plant are shown in Table 1. Also the turbine/generator assembly is shown in Fig. 1.

This power plant is located in Japan's central mountainous area, at an elevation of over 1,400m, surrounded by numerous steep mountains. This report introduces the following new techniques adopted to overcome these unfavorable construction conditions and to make the power plant more economical.

(1) High specific speed design of 6-jet Pelton turbine
(2) Elimination of bypass
(3) Electrically powered deflector/needle operating mechanism

Table 1 Turbine/generator specifications for Nikengoya Power Plant

Turbine	Type	Vertical shaft 6-jet Pelton turbine
	Net head	283.6m
	Discharge	11.0m³/s
	Output	26,800kW
	Rated speed	400r/min
Generator	Type	3-phase vertical synchronous generator
	Cooling	Totally enclosed (Machine mounted heat exchanger type)
	Output	27,400kVA
	Voltage	11kV
	Current	1,439A
	Power factor	95% lag
	Frequency	60Hz
	Rated speed	400r/min

2. High Specific Speed Design of 6-Jet Pelton Turbine

2.1 Background of high specific speed design

Located in a secluded mountainous area, this power plant imposed extremely severe limits on transportation. Therefore, minimizing the size of the turbine/generator was the most important matter in planning this power plant. In addition, since minimi-

Fig.1 Turbine/generator assembly

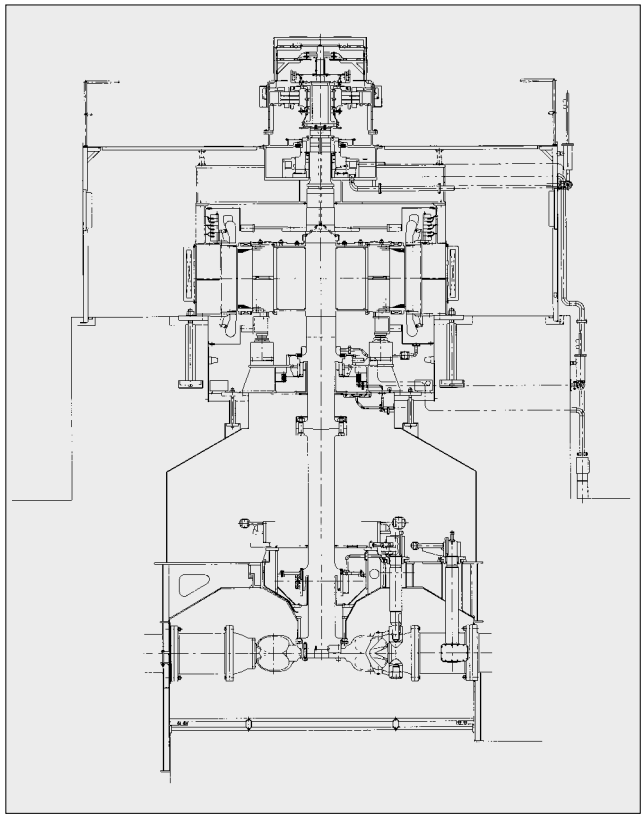

Fig.2 Relative efficiency of conventional and new model

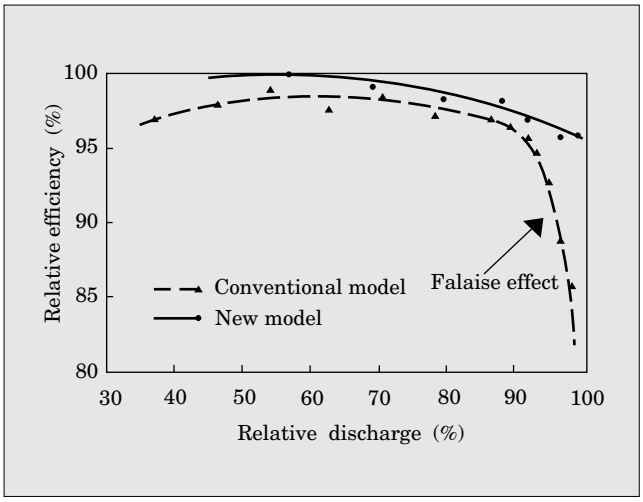

Fig.3 Bypass in run-of-river plant

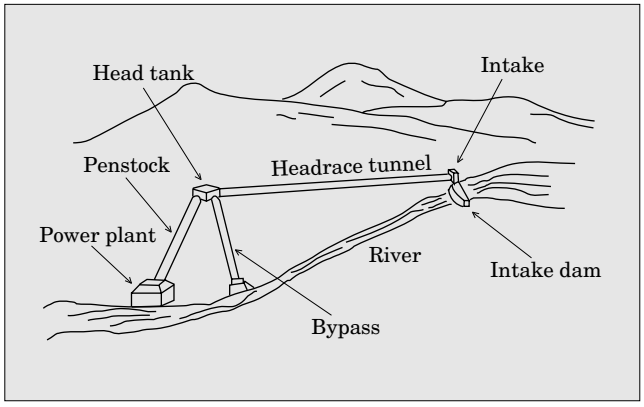

Fig.4 Deflector start-up characteristic at the field test

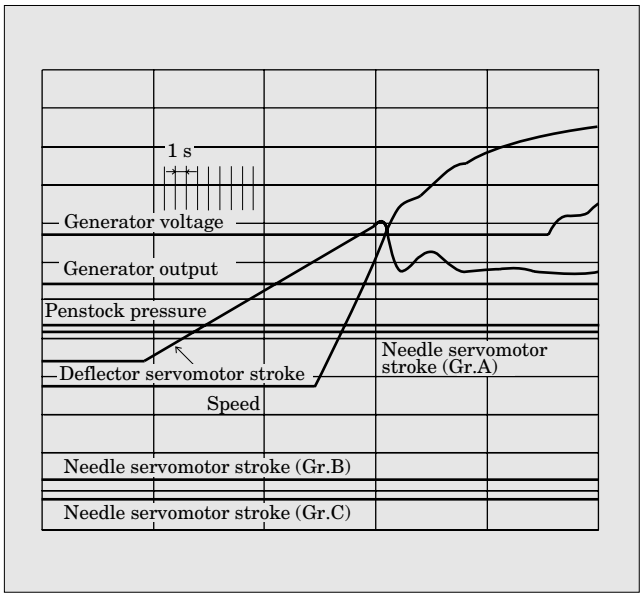

zation of the turbine/generator not only lowers the cost of equipment but also reduces the powerhouse size, construction costs of the power plant can also be reduced. Therefore, for this power plant, the turbine was designed to have as high specific speed as possible so as to make the equipment more compact, satisfy the transportation limit, as well as to make the power plant more economical.

The specific speed of a Pelton turbine is generally expressed with the following equation.

$$n_s = \frac{n\sqrt{P/Z}}{H^{5/4}} \quad \cdots\cdots (1)$$

Where, n_s : Specific speed (m-kW)
n : Speed (r/min)
P : Turbine output (kW)
Z : No. of jets
H : Net head (m)

As is clear from the definition of specific speed, it is necessary to increase the number of jets and the turbine speed in order to increase the specific speed. However, it is well understood that when the number of jets is increased to, for example 5 or 6 jets, a problem with turbine performance – known as the falaise effect – will occur. This effect has never been a matter of concern when the number of jets is less than 4. For this reason, it is an international practice to limit the specific speed of a 6-jet Pelton turbine to approx. 20 m-kW or less.

The problems of this falaise effect have been improved and the result, as applied to this power plant, is described below.

2.2 Falaise effect

Figure 2 shows the relative efficiency of a conventional model which exhibits the falaise effect, and of a new model with improved falaise effect. As this figure clearly shows, when the falaise effect occurs in a full load region, it will lead to a considerable drop in turbine efficiency. In this region, power swings and erosion of the bucket's inner surface will also occur. Therefore, the falaise effect must be eliminated from the actual turbine operation region.

The mechanism of this falaise effect occurrence was analyzed by the observation of flow in model test and by numerical analysis. It was confirmed that there are 2 kinds of mechanisms for the occurrence of the falaise effect.

2.2.1 Falaise effect due to jet interference inside bucket

Jet interference, already a known cause, occurs when the next jet begins flowing into the bucket before water has completely flowed out of the bucket's leading edge, and these two jets violently collide in the bucket. As a result, a considerable hydraulic loss occurs inside of the bucket.

2.2.2 Falaise effect due to jet interference outside bucket

This is a newly discovered type of jet interference, where water flow from a cut-out area, interferes with the next jet which has not yet entered the bucket. As a result, the jet becomes turbulent, scatters and loses its energy before flowing into the bucket.

Further, in this high specific speed design study, a

comparative analysis was also made in the falaise effect region between the measured results of prototype performance and those of the model test. Although several studies[1] have been made on the efficiency scale effect from model to prototype, so far there is no established theory. We had the opportunity to examine the efficiency scale effect in a Pelton turbine from model to prototype including its relation to the falaise effect mechanism[2].

2.3 Reducing the falaise effect

To counteract the previously described mechanisms, the following design was applied to this plant to reduce the falaise effect.

2.3.1 Improved bucket configuration

The tendency of the jet output to flow toward the leading edge of bucket was controlled by improving the bucket wall slope and the shape of the cut-out area.

2.3.2 Relatively larger bucket size

By selecting a relatively larger sized bucket, the tendency to flow toward the cut-out area of the bucket was reduced.

2.3.3 Increased number of buckets

By increasing the number of buckets, the time for each bucket to receive the jet can be reduced.

With these design philosophies, a high specific speed design (n_s = 23.0m-kW) was successfully achieved for the first time in the world.

3. Elimination of Bypass

3.1 Bypass in run-of-river plant

At run-of-river plant, river water flow into a power plant through an intake dam and used as is for power generation. If the power plant is shut down or the amount of river water taken in becomes excessive, the bypass, as shown in Fig. 3, directly discharges such excess water from the head tank to the river, bypassing the power station. Therefore if this bypass can be eliminated, construction costs will be reduced by a large percentage of the overall power plant construction cost.

Since the elimination of a bypass will result in problems such as a rise of the river water level due to closing of the intake gate, pressurization of the headrace, etc., the installation of a bypass or similar substitute has been required at run-of-river plants by a Japanese statute. However, application of a Pelton turbine will make it possible to eliminate the bypass, as the above-mentioned problems can be avoided by deflector discharge operation for long periods of time and implementing start/stop controls with the deflector.

3.2 Basic concept of bypass elimination

The basic concepts for eliminating a bypass for a Pelton turbine are as follows:

(1) The intake gate shall be controlled such that the rate at which the river water level rises is small.
(2) The turbine will perform a full flow deflector discharge operation.
(3) When malfunctions of the transmission line are not recovered within a specified time, and when malfunctions of the generating unit occur, the intake gate shall close.
(4) When malfunctions of the transmission line are recovered within a specified time, the generating unit shall automatically begin operation again in parallel.

3.3 Technical outline of bypass elimination

For the previously mentioned basic concepts of bypass elimination to be realized, the civil, electrical and mechanical equipment must take on new functions. An outline of bypass elimination techniques with regard to electrical and mechanical equipment is described here.

3.3.1 Deflector discharge operation over a long period of time

During the deflector discharge operation, after high speed jets directly hit the deflector, they spray around the deflectors, hitting the housing, nozzle protection shield, etc. Therefore, after studying the strength and rigidity of these parts, the plate thickness was increased by approximately twice the existing thickness of these parts.

To verify the reliability of a deflector during discharge, the most severe operating condition, in addition to analytical studies on papers, the actual stress was measured beforehand on an identical prototype turbine. These results were reflected in the design of this power plant.

3.3.2 Start/stop controls by deflector

In conventional Pelton turbines, starting and stopping the generating unit was controlled by needles, and the deflector performed follow-up control. However, in the case of bypass elimination, needles will only control the head tank water level regulator and start/stop controls will be performed by the deflector. To implement such deflector control, the following studies were made.

(1) Reduction of hydraulic torsional moment of deflector

In a 6-jet Pelton turbine with push-out deflectors, when starting and stopping a units, a jet which deflected by an adjacent deflector will hit the rear surface of a deflector. This causes the hydraulic torsional moment of the deflector to sharply increase. Therefore, models were tested to optimize the configuration, size and installation position of the protecting shield, so as to eliminate this collision between jet and deflector rear surfaces. As a result, the hydraulic torsional moment of the deflector and the capacity of the deflector servomotor can be reduced.

(2) Numerical analysis of deflector start operation

The optimization of a governor setting was made

Fig.5 Deflector operating mechanism

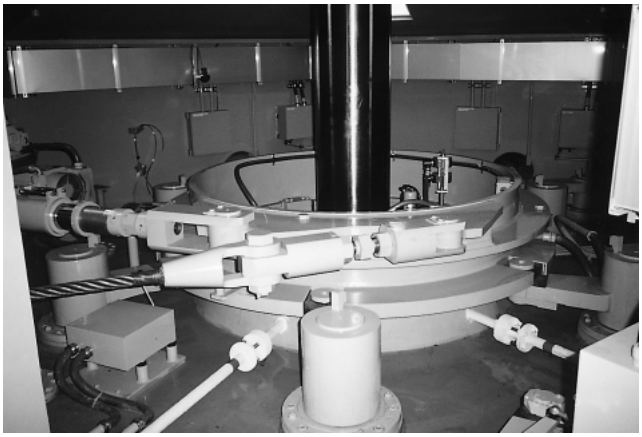

Fig.6 Electric deflector servomotor

by analyzing with a stability calculation program, the stable deflector start operation regardless of needle opening and nozzle combination.

From the result of the above studies, a stable start-up characteristic, as shown in Fig. 4, by a deflector was obtained at the field test.

3.3.3 Deflector and needle functions

There are two requirements for eliminating the bypass. First, the headrace tunnel should not be pressurized regardless of the type or severity of accident, and secondly, the water should not overflow from the head tank. Therefore, in case of a drop in or loss of power supply voltage during operation, the deflector and needles must be able to securely carry out the following operations.

(1) The deflector should be able to fully close and switch to the deflector discharge operation independent of the electrical signals.
(2) Needles should maintain the current opening.

These functions were added to the electrical servomotor described in the next section.

4. Electrically Powered Deflector/Needle Operating Mechanism

4.1 Background of electrical power

In convention hydropower plants, the oil pressure servomotor was adapted as the operating mechanism for the turbine. However, the oil pressure servomotor requires auxiliary equipment such as oil pressure supply equipment, oil pressure piping, etc. and a considerable amount of time was spent maintaining and inspecting this equipment. In particular, as Pelton turbine construction sites have become increasingly remote in recent years, there is a strong demand for reduced maintenance and inspection of this equipment.

Under these circumstances, the deflector/needle operation mechanism of the 6-jet Pelton turbine for this power plant was electrically powered for the first time in Japan, and the entire hydraulic oil pressure system was eliminated As a result, not only was the initial equipment cost reduced but the maintenance cost, or in other words, the operating cost was also reduced.

4.2 Electrically powered deflector operating mechanism

The 6 deflectors are connected to a guide ring, via the deflector shaft, by a slider block type linkage mechanism. The guide ring is connected to an electric servomotor and to a counter weight for emergency closure. A guide ring using a slider block is newly developed, the application of which has resulted in the simplification of the conventional complex linkage mechanism that utilized turnbuckles. Figure 5 is a photograph of this deflector operating mechanism.

Specifications of the electric deflector servomotor are as follows:

Rated load : 156,900 N
Closing and opening time : 15 s
Maximum stroke : 250 mm
Motor output : 11 kW
Motor voltage : 200V AC
Motor speed : 1,000 r/min

As mentioned in the section on bypass elimination techniques, the electric deflector servomotor is connected to a counter weight for emergency closure so as to be able to close the deflector independently of electrical signals in case of a drop in or loss of power supply voltage. A photograph of this electric deflector servomotor is shown in Fig. 6.

4.3 Electrically powered needle operating mechanism

Each of the 6 needles is connected by a linkage mechanism, via the needle shaft, to 6 electric needle servomotors that can be operated independently. A special feature is the use of a slider block in the nozzle pipe to convert rotating motion of the needle shaft to linear motion.

The specifications of each electric needle servomotor are as follows:

Rated load : 58,800 N
Closing and opening time : 30 s
Maximum stroke : 205 mm
Motor output : 1.5 kW
Motor voltage : 200V AC
Motor speed : 1,000 r/min

As stated in the section on bypass elimination technique, since the electric servomotors must maintain the current opening regardless of a drop or loss of power supply voltage, they are equipped with a magnetic brake. This type of magnetic brake is free when energized and brakes when released to operate securely under emergency conditions.

4.4 Power supply system

An uninterruptible power unit is provided to supply power to one electric deflector servomotor, 6 electric needle servomotors and the magnetic brake.

This system supplies alternating current (200V AC), through a rectifier and inverter, as power at the rated voltage and frequency. In case of a drop in AC voltage or power outage, a battery will supply the power. In addition, this system has a bypass circuit in case failures occur in the inverter. Should such a failure occur, the bypass circuit will be switched on automatically to deliver the AC current directly and without interruption.

This system will provide each electric servomotor with electrical backup functions, which in addition to mechanical backup functions (counter weight for emergency closure and magnetic brake) improve the overall reliability of the system.

5. Conclusion

The latest technologies applied to the vertical 6-jet Pelton turbine of the Nikengoya Power Plant were introduced above. We expect that these new technologies for the Pelton turbine will be efficiently adapted in future plans for hydropower plants and that these technologies will continue to develop.

We are most grateful to all the parties concerned who advised and cooperated with us from the planning, design, and site installation phases through testing of this plant.

References:

(1) H. Grein, et al.: Efficiency Scale Effects in Pelton Turbine, IAHR Symposium (1986)
(2) T. Kubota, et al.: Scale Effect on a 6-Nozzle Pelton Turbine, 7th International Seminar Water Energy Plants, Wien (1992)

Recent Analysis Technologies for Hydropower Equipment

Kentaro Akahane
Ryoji Suzuki

1. Introduction

Computers are being used at each stage of hydropower equipment setup, from the receipt of a purchase order to onsite installation and testing.

The history of analysis technologies for hydropower equipment began with the introduction of flow analysis technology into runner design and has developed as computers have increased in speed and capacity. This analysis has made the transition from the classic performance improvement technique based on model tests using the try and cut method to computer-aided flow analysis and performance prediction technologies. Also, with the increase in the dimensions and head of hydraulic turbines, a strength and vibration analysis technique has been introduced. This technique contributes to the optimum construction design of hydraulic turbines. Presently, various numerical analysis technologies are used at each stage of hydraulic turbine planning and design.

This paper outlines the analysis technologies commonly used for hydropower equipment.

2. Flow Analysis Technologies

Flow analysis as a design tool for hydraulic turbines and reversible pump-turbines began in the 1960s with two-dimensional, inviscid flow analysis, and continued in the 1970s with quasi-three-dimensional analysis. The quasi-three-dimensional method divides a flow passage into many rotating flow surfaces of axial symmetry and performs iterative calculations, repeating the flow analysis for each flow surface and modifying the profile of the flow surface using each analysis result. Because this method requires only a comparatively small memory capacity and can be calculated quickly, it is still used as a simple design tool. However, this method is based on the approximation that fluid flows on a rotating flow surface having axial symmetry, and is insufficient to describe the details of much more complicated flows in actual hydraulic turbines and reversible pump-turbines. For example, it is known that flow over the pressure surface of high-specific-speed Francis runners used for low head projects is approximately perpendicular to the rotating flow surface, but this flow phenomenon can not be described by the quasi-three-dimensional method. In addition, because of recent demand for stable operation not only at the point of optimum efficiency and its vicinity but also over a wider range, the necessity to describe the internal flow at an operating point far from the design point has increased. The quasi-three-dimensional method has poor convergence in calculating these conditions, and little detailed information about the flow can be obtained from analysis with this method.

Using recently introduced three-dimensional viscous flow analysis technologies, complex flow phenomena in hydraulic turbines have become understood and the accuracy of analysis in regions far from the design point has greatly improved. Many flow phenomena are being clarified, such as the flow separation occurring in a runner during high-head and low-head operation or the channel vortex in partial load operation, the leakage flow from the blade tip clearance of a Kaplan turbine, and the reverse flow at the inlet of a reversible pump-turbine during high-head pumping operation. This progress in analysis technologies has made it possible to obtain more detailed information at the design stage than ever before.

On the other hand, the preparation of data for analysis and those analysis calculations require much more time than the previous quasi-three-dimensional analysis. Therefore, quasi-three-dimensional analysis and three-dimensional viscous flow analysis are properly used in combination at present.

The progress of flow analysis technologies has improved design accuracy and reliability. The previous method in which performance was improved by repeating model tests is gradually changing to a method in which the optimum design obtained from iterative flow analyses and then confirmed with a model. However, to completely eliminate model tests, strict direct numerical simulation of Navier-Stokes equations must be easily performed on desktop computers and the accuracy and reliability of these results must be recognized generally. These expectations are

unrealistic at the present time. It should be noted that the model test is an effective method to verify the result of analysis. The flow analysis technologies are powerful because they quantify elements previously dependent on the designer's perception and sense and promote progress in design technology. These analysis technologies will contribute to expanding the stable operation region of hydropower equipment by shifting the range of instability or by controlling the strength of that phenomenon.

3. Strength Analysis Technologies

As described above, with the increase of computer speed and capacity, the finite element method (FEM) which had been previously impractical because of its enormous quantities of calculations became calculable in two-dimensions beginning from approximately 1970 and in three-dimensions from the mid 1970s. This technique also was applied to strength analysis of the main structures of hydraulic turbines and reversible pump-turbines. First, it was mainly used for structures having two-dimensions or axial symmetry with simple shell elements and beam elements, and then gradually became used in complicated, large-scale analyses with three-dimensional solid elements. It has been applied not only to simple supports or immovable restraints but also to constraint conditions closer to actuality, such as multipoint constraint. Recently, FEM analysis has been easily performed with desktop engineering workstations or personal computers. Static and dynamic stress and displacement are more precisely calculated, greatly contributing to improved equipment reliability, including fatigue strength.

It is important that each part of a high-head hydraulic turbine or reversible pump-turbine has the necessary stiffness to endure high water pressure. The FEM also handles nonlinear phenomenon such as the rapid increase in bolt tensility caused by opening a flange fastened by large bolts. In contrast, low-head bulb turbines have a large thin plate structure and it is important to predict the precise amount of deformation under manufacture, assembly, and installation. Our method of onsite installation is based on the result of analyzing deformation during operation.

4. Vibration Analysis Technologies

Eigenvalue analysis with FEM is generally performed to eliminate resonance problems.

Reversible pump-turbines often have a high head and large capacity to improve economical efficiency. They also require high reliability. Because a high head increases the exciting force of water pressure on the parts, an analysis of vibration in the water is necessary for the runner. A fluid reaction force proportional to the acceleration of vibration acts on the runner in the water and exerts the effect of additional mass, which lowers the natural frequency. The runner is also influenced by the stationary head cover and bottom cover. Therefore, it is necessary to perform fluid-structure-coupled vibration analysis that includes fluid around the runner and the stationary parts, and to ensure that the frequency of fluctuating stress is sufficiently far away from the resonance frequency. At present, verification is carried out both through analysis with software and the measurement of fluctuating stress at an actual head testing facility.

On the other hand, low-head bulb turbines have low stiffness and their natural frequency is low. Therefore, eigenvalue analysis is performed for the whole model.

A special example is the verification of the effectiveness of a pump-turbine structure for reducing building vibration. Vibration analysis of the building structure of a certain high-head, pumped-storage power station was performed. The analysis result agreed favorably with onsite measured values.

5. Transient Phenomenon Analysis Technologies

The analysis of transient phenomena in hydraulic turbines, especially the calculation of pressure rise (ΔP) and speed rise (ΔN) during load rejection, and the required flywheel effect (GD^2) that influence not only the preservation of the hydroelectric power plant building and equipment but are also directly related to the cost, is always carried out during estimation and planning stage. In other words, a method of closing guide vanes to minimize the required GD^2 while maintaining ΔP and ΔN within permissible tolerance is investigated. When a tailrace is formed by a long pressure tunnel, there is a possibility that pressure during load rejection will drop to the vapor pressure level (known as the water column separation phenomena) causing an abnormal pressure rise during the reattachment of water columns. Therefore, it is necessary to simulate water pressure behavior. In addition, analysis may be necessary in a complex waterway system such as where a penstock branch and a surge tank are combined to confirm stability of the governor control.

6. Conclusion

An outline of the history and recent analysis technologies of Fuji Electric's hydropower equipment has been presented. Other papers in this special issue introduce "Vibration Analysis Technologies for High Head Pump-Turbine Runners" and the "Application of Numerical Flow Analysis Technologies to Hydraulic Turbines and Pump-Turbines". We would be grateful if you would take the time to read them.

Vibration Analysis Technologies for High Head Pump-Turbine Runners

Ryoji Suzuki
Yutaka Kimoto
Masayoshi Sakata

1. Introduction

In the early 1970's, the head exceeded 500 meters in pumped storage power plants in Japan. But for a more economical construction, a higher head was pursued. Recently, higher rotational speed and more compact equipment have been adopted. Among the many technical subjects in the planning and design of high head pump-turbines, the estimation of dynamic stress on the runners is most important in realizing highly reliable runners. With higher speed and a higher head, not only static stress on the runner but also dynamic stress and its frequency increases. This is because the amplitude and frequency of the pressure pulsation around the runner increase. Therefore, in the design stage, the technology for prediction of dynamic stress acting on the runners is of major importance.

In accordance with these technical requirements, Fuji Electric has developed fluid-structure coupled vibration analysis technology and an actual head model test apparatus. In this paper, these developments will be briefly described.

2. Vibration Characteristics of the Runner in Water

As the runner blades of a pump-turbine in generating mode pass one by one through the wakes of the guide vanes, velocity and pressure around the blades fluctuate periodically. In pumping mode, velocity and pressure around the blades also fluctuate as the blades approach and pass the guide vanes. Such pressure pulsation due to the interaction between stationary and rotating cascades varies according to the combination of the number of blades. This pressure pulsation generates a pressure field with diametrical nodes satisfying the equation;

$$n \cdot Z_G + k = m \cdot Z_R \quad \cdots\cdots (1)$$

Where Z_G and Z_R are the number of guide vanes and runner blades, respectively, and n and m are orders of excitation. The symbol k is the number of diametrical nodes which corresponds to the vibration mode. This is illustrated in Fig. 1.

Fig.1 Vibration modes of a disk with various diametrical nodes

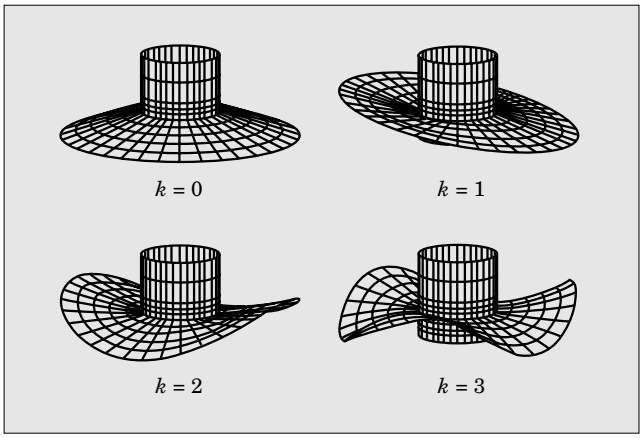

The frequency of pressure pulsation acting on the rotating runner is;

$$f_R = n \cdot Z_G \cdot N / 60 \quad \cdots\cdots (2)$$

Where N denotes the rotating speed of the runner (r/min). Such a pressure field with diametrical nodes rotates with a speed of;

$$f_{PR} = f_R / k \quad \cdots\cdots (3)$$

Where positive k corresponds to a progressive wave, a wave rotating in the same direction as the runner, and negative k corresponds to a reverse wave, a wave moving in the opposite direction as the runner.

The frequency and the rotational speed of the pressure pulsation observed on the stationary parts are;

$$f_S = m \cdot Z_R \cdot N / 60 \quad \cdots\cdots (4)$$

and

$$f_{PS} = f_S / k \quad \cdots\cdots (5)$$

In addition, although there are infinite combinations of n, m and k satisfying equation (1), the specific mode of the pressure field which actually cause the vibration on the runners can be found. Taking into account the response of the runner excited by such a pressure pulsation, the following conditions can be drawn:

(1) Lower order excitation modes (smaller n) generally cause a larger response on the runners.
(2) Excitation modes with smaller k generally cause larger response on the runners because they excite

vibration with less diametrical nodes.

(3) A pump-turbine runner consists of two disks (crown and band) connected by blades, and thus responds easily to the excitation by which the displacement at blade roots can always be zero.

The first and second conditions, specify modes with $n = 1$ and smaller $|k|$. From the third condition, it can be concluded that the combination of two modes are specified, of which the difference in k is equal to the number of runner blades. Table 1 lists the combinations of excitation modes for various numbers of runner blades and guide vanes which are obtained by such an investigation. For example, a pump-turbine with 20 guide vanes and 6 runner blades is subject to excitation with 2 and 4 diametrical nodes. In this case, the pressure pulsations with frequencies of 3 and 4 times $Z_R \times N$ are observed on the head cover. Excitation of the first order on the runner has a frequency of $Z_G \times N$ in all cases.

When the resonance frequency of a pump-turbine runner is numerically analyzed, the above-mentioned excitation mode should be considered. Because the vibration caused on a runner by the interaction with guide vanes has a relatively high frequency, many natural frequencies are obtained below the modes in question. The result should be evaluated, taking into consideration that the mode with the same number of diametrical nodes as the excitation mode is selectively amplified.

3. Coupled Vibration Analysis in Water

3.1 Analysis method and calculation model

It is a well-known fact that the natural frequency of a structure in water generally varies from that in air. The natural frequency of a structure in extensive water is reduced by around 20%. This reduction in natural frequency is caused by the added mass effect, which is due to the reaction force (pressure) from the water adjacent to the structure. This reaction force is proportional to the acceleration of vibration.

In the case of a pump-turbine runner, there are small spaces between the crown and head cover and between the band and bottom cover. When the crown and the band vibrate, the water in these spaces must move peripherally or move out of the space through the runner seal and the outer periphery. The volume of this water is determined by the displacement of the crown and the band. Therefore, the reaction force from water, or the added mass effect, of the runner is much larger than in extensive water. Therefore, the natural frequency of pump-turbine runners in operation is reduced by around 50% that of air. Because this reduction rate is affected by the mode shape of vibration, the space between the head/bottom covers and the runner, the stiffness of the head cover, etc., numerical analyses are necessary in order to quantitatively predict the natural frequency in the design stage.

Table 1 Excitation mode on the runner (number of diametrical nodes)

Z_R \ Z_G	16	20	24
6	−4 / +2	−2 / +4	−6 / 0 / +6
7	−2 / +5	−6 / +1	−3 / +4
8	−8 / 0 / +8	−4 / +4	−8 / 0 / +8
9	−7 / +2	−2 / +7	−6 / +3
10	−6 / +4	−10 / 0 / +10	−4 / +6

Vibration analysis of the runner is carried out using the solver provided by MSC/NASTRAN, which calculates the added mass effect of fluid. As the boundary element method is used for the solution of the fluid property, the definition of the boundary is only required for the modeling of the fluid region. But a knowledge of the definition of the fluid boundary is necessary. In addition, it takes a long time for the solution of simultaneous equations. This is because a full matrix is produced for the fluid region due to the application of the boundary element method. As a result, modeling knowledge has been accumulated through the comparison between calculated and measured vibration modes based on such systems as a simple disk in a vessel.

Figure 2 shows the analytical model of a pump-turbine runner. To take into account the effect of the gap between the runner and the head/bottom covers and the stiffness of the head cover, the model includes the head and bottom covers.

3.2 Example of analysis results

Figure 3 shows an example of the vibration mode and stress distribution of a runner. Many natural frequencies with various vibration modes are obtained by the fluid-structure coupled vibration analysis solver in MSC/NASTRAN. As mentioned above, the degree of response is different for each mode because of the specific mode of the pressure pulsation acting on the runner in operation.

Hence, the modal response analysis is carried out

Fig.2 Finite element analysis model of a pump-turbine runner

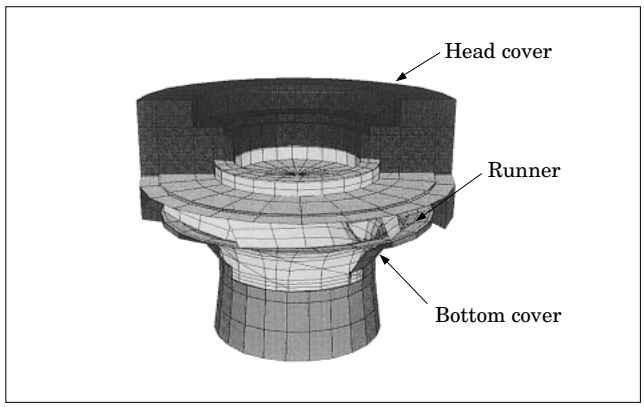

Fig.3 Vibration mode and stress distribution on the runner

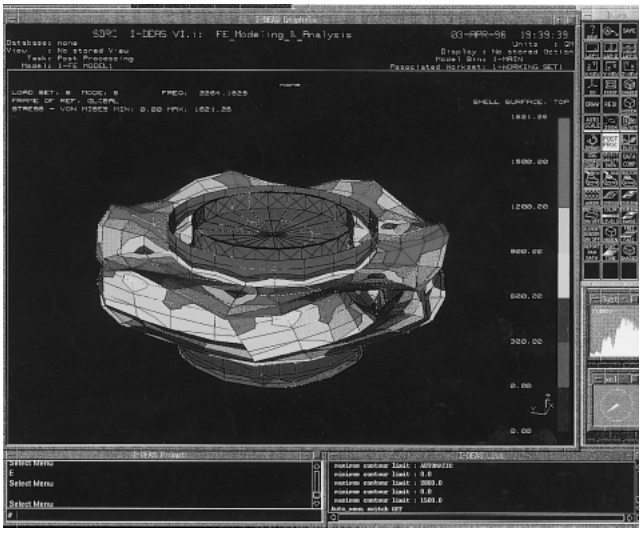

Fig.4 Flow chart of mode synthesize method program

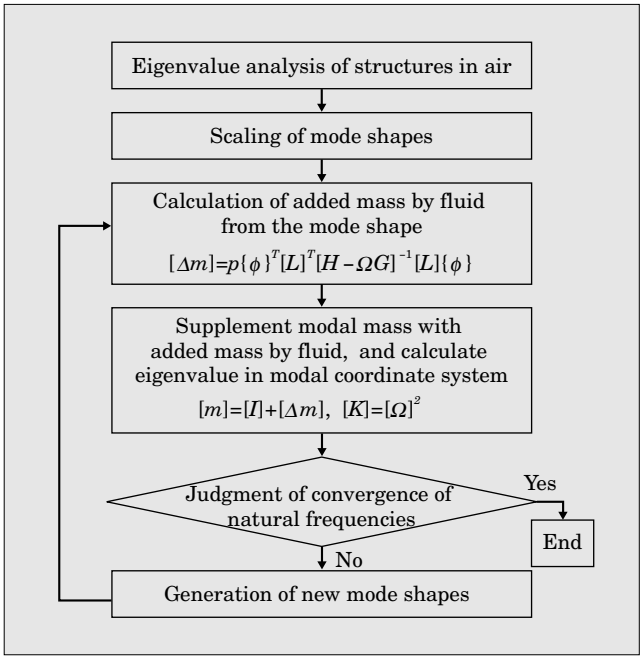

Fig.5 Actual head model test stand

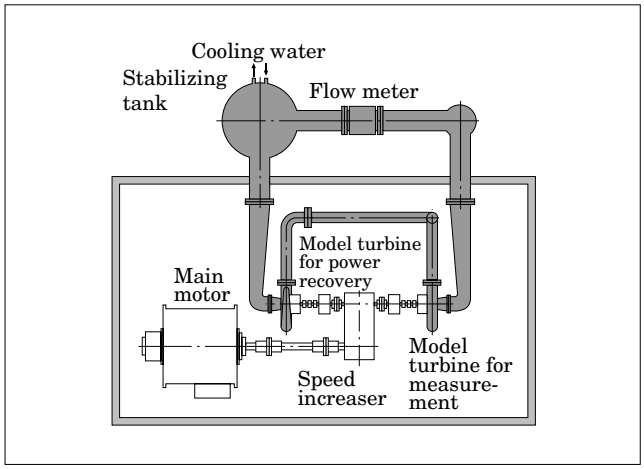

by applying pressure pulsation on the runner, based on the result of fluid-structure coupled vibration analysis, in order to predict the actual natural frequency. Then, the level and location of dynamic stress can be quantitatively estimated from the stress analysis according to the amplitude of vibration. Because the absolute level of pressure pulsation as well as the dumping factor are difficult to directly calculate, the reliability of calculation is improved by feedback of the measured data in the power plants and the actual head model test stand.

3.3 Fluid-structure coupled vibration analysis method by mode synthesize method

As the fluid-structure coupled vibration solver in MSC/NASTRAN applies the boundary element method for the fluid region, it has the advantage of easy mesh generation. At the same time, its disadvantages induce long calculation time and structural modeling limited by the shell elements. In order to eliminate such defects, a new fluid-structure coupled vibration analysis code was developed using the mode synthesize method.

This method is based on the governing equations of unstable pressure distribution caused by small scale vibration of compressible fluid. The equation of motion for structures are coupled with fluid elements by introducing in the external force term the pressure generated by the vibration of the wall facing the fluid region. If the simultaneous equations are solved directly, a very large matrix with a combination of structures and fluid regions is generated. Thus, the algorithm shown in Fig. 4 is applied to reduce calculation time.

By this method, the eigenvalue analysis of the structures in air is carried out first. Then, the force acting on the fluid is calculated using the mode of vibration normal to the wall. Consequently, the pressure pulsation, generated by this external force, acts on the structure. As this pressure pulsation is proportional to the acceleration of the wall, it is equivalent to the added mass on the boundary wall. These added mass components are calculated by the mode synthesize method based on the vibration mode of the structure. These algorithms are iterated until the natural frequencies converge.

4. Dynamic Stress Measurement in Actual Head Model Test Stand

4.1 Actual head model test stand

As stated above, a pump-turbine runner rotating in water forms a coupled vibration system due to its interaction with the surrounding water and structures. In order to simulate such a coupled vibration phenomenon using a model, the hydroelastic similarity law must be satisfied. In other words, the ratio of

hydraulic excitation frequency to the natural frequency of the runner should be equal for both the prototype and the model. In the case of a pump-turbine runner, this similarity can be satisfied by manufacturing the model runner with the same material as the prototype and by operating the model runner with the same peripheral speed, or with the same head, as the prototype. Under such conditions, vibration observed in the model has a frequency in inverse proportion to the scale ratio and the amplitude is nearly similar to the prototype, if a small discrepancy in damping due to the difference in the Reynolds number is overlooked.

The actual head model test stand is the facility for the above-mentioned purpose and is outlined in Fig. 5. The torque generated by the main motor is transmitted to the model turbine through the speed increaser. The maximum available speed of the model is more than 7,000 r/min. In spite of the small scale model, a few MW of input power is required for hundreds of meters of test head; thus, this facility is equipped with a pair of model turbines at both ends of the high speed shaft. When one of the models is operated in pumping mode, the other recovers the driving power through the generating mode operation. Figure 6 portrays the model test facility in operation.

4.2 Example of measurement in actual head test stand

Stress measurement was carried out in this test stand with the model designed for a 400m class pumped storage power plant. The principal specifications of the prototype are listed below.

(1) Type : Reversible Francis pump-turbine
(2) Net head : 400m
(3) Max. output : 360MW
(4) Speed : 360r/min
(5) No. of runner blades : 6
(6) No. of guide vanes : 20

The stress on the runner was measured by 12 strain gauges, each of which was monitored simultaneously by a 12 channel FM telemeter. Together with the stress, operating conditions such as the rotating speed of the runner, discharge and static pressure at the inlet and outlet of the model were also measured. Preceding the installation of the strain gauges, finite element analyses were carried out in order to determine the location of maximum stress for the assumed

Fig.6 Actual head model test stand in operation

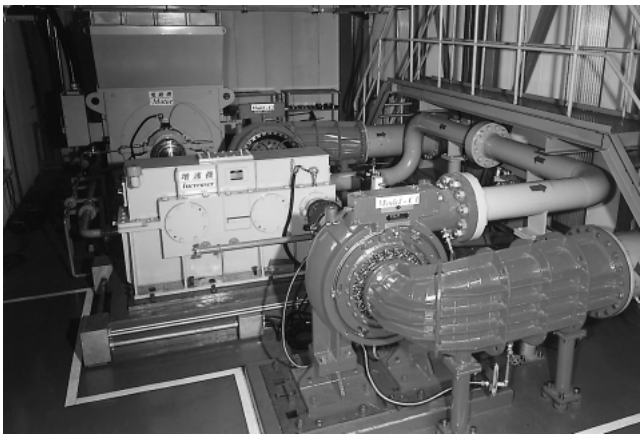

Fig.7 Measured stress amplitude on the runner in generating mode

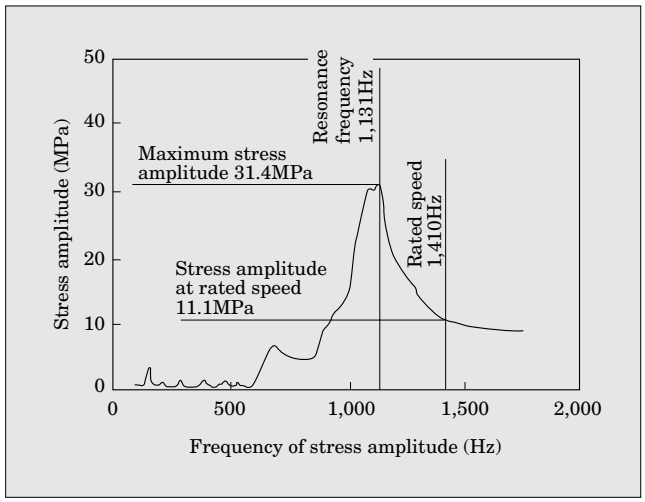

Fig.8 Measured stress amplitude on the runner in pumping mode

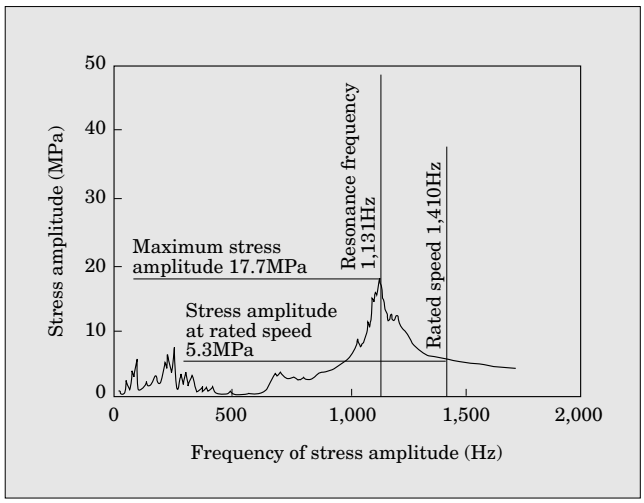

Fig.9 Comparison between analyzed and measured stress amplitude (generating mode)

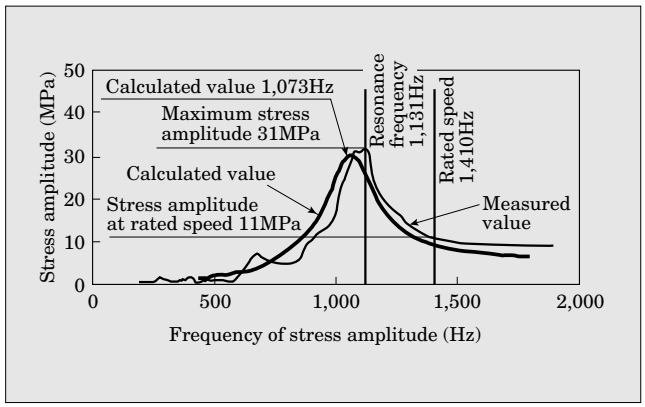

vibration mode.

Figure 7 shows the amplitude of dynamic stress as a function of frequency in generating mode, which is measured by changing the rotational speed continuously. An obvious peak can be seen at 1,131Hz, and the maximum stress amplitude at the resonance point is 31.4MPa. The frequency of hydraulic excitation of the prototype rotating with the rated speed of 360 r/min corresponds to 1,410Hz on the model. Therefore, the prototype is operated at a frequency 20% different from the resonance frequency, where the stress amplitude is 11.1MPa, or 1/3 of peak value.

Figure 8 shows the stress amplitude measured during pumping operation. An obvious peak exists at 1,131Hz, the same as in the generating mode, but the level of the stress amplitude is about half that in the generating mode including the resonance point. This is because the hydraulic excitation due to the interaction between the guide vanes and runner blades is less than in generating mode.

From these measurements, it is confirmed that the level of the stress amplitude for the prototype's operating conditions is sufficiently low compared with the strength of the runner in both the generating and pumping modes.

4.3 Comparison of the results of coupled vibration analysis

Figure 9 shows the results of the modal response analysis in generating mode based on the fluid-structure coupled vibration analysis compared to measurements taken during testing with the actual head model. The resonance frequency of the runner obtained by the analysis is 1,073Hz, while the measured frequency is 1,131Hz, as stated above. The error of numerical prediction is about 5%, and accuracy is sufficient for practical use. In addition, simulated stress amplitude as a function of frequency also coincides well with measurements. It is confirmed that the stress amplitude acting on the runners can be predicted in the design stage with sufficient accuracy, and that a design that avoids resonance is possible.

5. Conclusion

In this paper, an outline of recent developments in the evaluation of vibration characteristics of pump-turbine runners in operation were reported. It was shown that the characteristics of dynamic stress on pump-turbine runners in operation can be estimated with sufficient accuracy before the manufacturing of prototypes. This was proven using both computer aided fluid-structure coupled vibration analysis technology and actual head model test technology.

The pumped storage power plants of the future will probably increase in both head and speed. Though the technical requirements become increasingly severe from the viewpoint of reliability for the vibration of the runners, we hope the technology presented here will contribute to further developments in the world of electric power generation.

Application of Numerical Flow Analysis Technologies to Hydraulic Turbines and Pump-Turbines

Yi Qian

1. Introduction

Numerical analysis technology has been widely developed as an important tool in engineering design due to the low cost and rapid development of Computer Technology (CT), especially in the Engineering Workstation (EWS) and Personal Computer (PC). In addition, the advancement of Computational Fluid Dynamics (CFD) technologies is also remarkable. A variety of new analytical techniques and turbulent flow models have been proposed and are now being applied to complicated flow analysis. Recently, several simulations with separation and swirl have been announced one after another, thereby expanding the range of application. Moreover, computer graphics (CG) technology has developed remarkably in recent years. This powerful drafting tool is used to visualize, in real time, analytical and data processing results on the computer display.

In this paper, the author introduces applications of the latest flow analysis technologies[(1)] to the design of hydraulic turbines and pump-turbines, and demonstrates the reliability and economy of the three-dimensional flow analysis technology.

2. Flow Analysis of Hydraulic Turbines and Pump-Turbines

2.1 Bulb turbines

A bulb turbine comprised of sixteen guide vanes and four runner blades is analyzed. The outline of the bulb turbine, which includes guide vanes, a runner and a draft tube, is shown in Fig. 1, and each operating condition is shown in Fig. 2. The optimum operating condition (on-cam) where cavitation at the runner entrance does not occur is made standard a point of computation (double circle). The computational domain extends from the inlet of the guide vanes to the draft tube exit, and the boundary conditions for the analysis include only discharge rate and head. To analyze the flow of this bulb turbine, two technologies are introduced.

2.1.1 Interaction between the rotor and stator

The guide vanes are stationary, and the runner blades are rotating. In fact, the flow patterns are three-dimensional and unsteady flow. If the computations are carried out by full, three-dimensional, unsteady flow, a very large computer and calculation costs become necessary to analyze the interaction phenomenon of this unsteady flow. In order to avoid these problems, previous researchers divided the computational area. That is, rotating and stationary blades were independently calculated, the interface between rotor and stator was disregarded. However, it

Fig.1 Outline and computational results of the bulb turbine

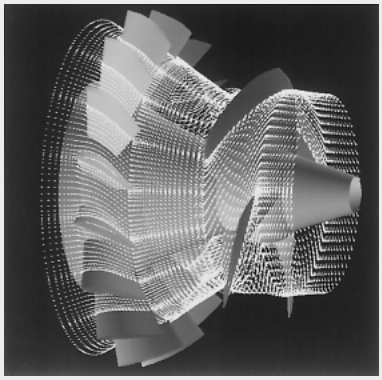

Fig.2 Discharge characteristics

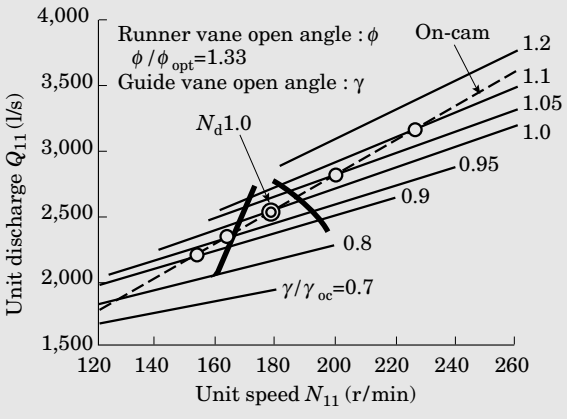

was confirmed that this divided calculation was different from the actual flow[3], and it was shown that the difference in the flow velocity distribution at the runner inlet was especially large. To evaluate the time average of a rotor-stator interaction correctly, the author proposed an approximate rotor-stator interaction analysis technique[2]. In this technique, the computational memory was decreased so that this computation could be carried out on a desktop EWS. Such techniques enable coupled analysis of the rotor-stator and use as a tool in hydraulic turbine design.

2.1.2 Leakage flow analysis technology

Leakage flow exists in the gap between the fixed discharge ring and rotating runner. When observing from the rotating runner, the leak flows from the pressure side of the blade tip gap toward the suction side. A local attack angle near the tip side at the leading edge is larger due to the effect of this leakage flow than in the case of disregarding the gap influence. The leakage flow from the blade tip gap strongly affects not only entrance cavitation performance but also downstream flow. Therefore, it is necessary to analyze the effects of leakage, taking the gap into consideration, to correctly evaluate the performance of the bulb turbine. As a result, the author developed the leakage flow analysis technique[2] which enables the leakage analysis of a very small gap.

2.1.3 Computational results

Three-dimensional flow simulation in a bulb turbine can be accurately carried out by introduction of the flow analysis technologies described above. Figure 1 shows the analytical results of a bulb turbine which includes guide vanes, a runner and a draft tube in optimum operating condition. The length of vectors corresponds to the magnitude of flow velocity. Figure 3 shows the distribution of flow velocity and pressure at the guide vanes' exit. Here, the ordinate represents the velocity components (C_z, C_θ and C_r) in the axial, circumferential, and radial directions, respectively. They are normalized by the runner's peripheral speed, and the pressure coefficient C_p is normalized by the dynamic pressures of the runner's peripheral speed. The pressure distributions on the pressure and suction surfaces of the runner blade at midspan are shown in Fig. 4, with the three lines representing three on-cam

Fig.3 Velocity and pressure distributions at the guide vanes' outlet

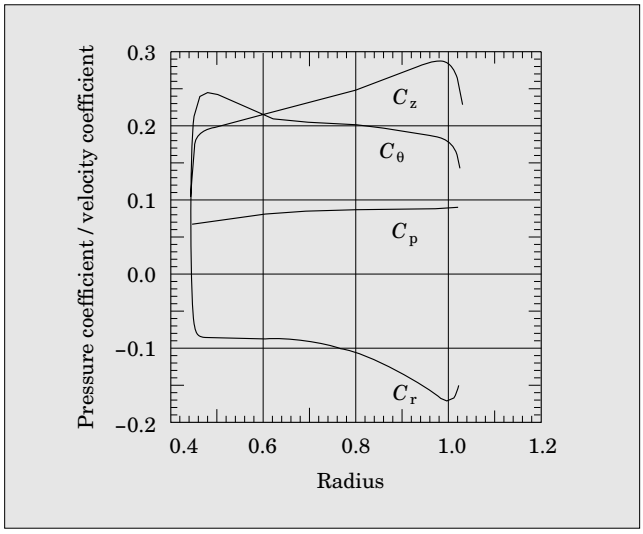

Fig.4 Pressure distribution on the bulb turbine runner

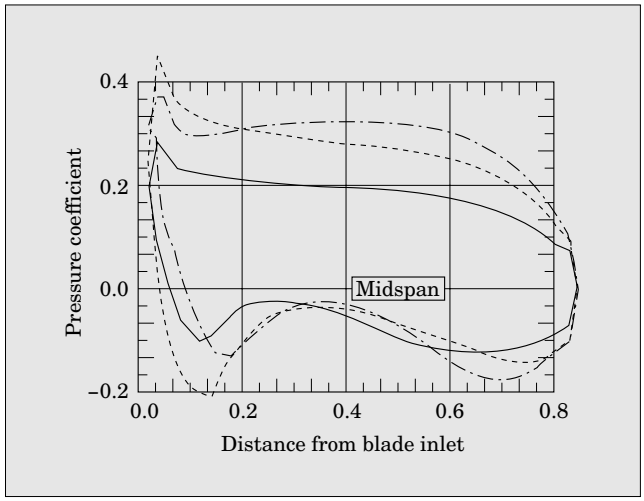

Fig.5 C_θ distribution by different passage forms upstream of the runner

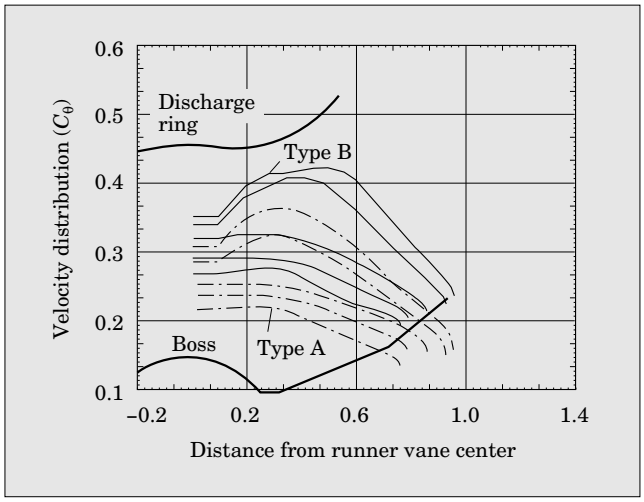

Fig.6 Outline and computational results of the pump-turbine

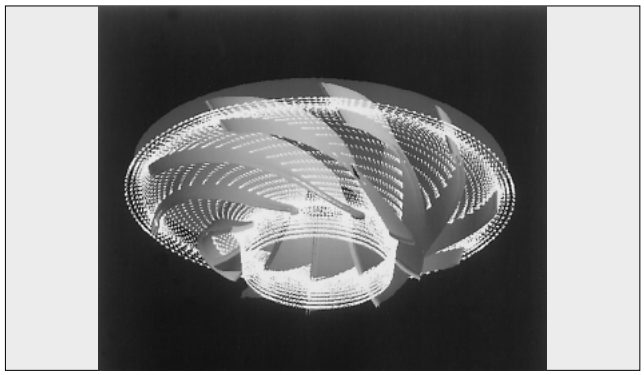

operating conditions.

In Fig. 5, the passage profile between the guide vane and runner is changed and then the distributions of circumferential velocity are compared from the boss to the discharge ring. It is understood that a difference exists in the absolute velocity and the spanwise spread of the velocity for both kinds of passages. The difference in velocity distribution directly affects the runner inlet flow condition. The best passage profile of such on-cam conditions can be chosen by flow analysis. These computational results will be very important in furthering runner design.

2.2 Pump-turbines

The pump-turbine operates the runner in either the forward or reverse direction and performs pump and turbine operations with one runner. Therefore, when the runner is designed, the performance of both pump and turbine operations must be considered. To improve the balance between pump and turbine performance, analysis of the flow of the pump-turbine in the design stage is much more important than the ordinary turbine runner.

Figure 6 shows the flow field in the blade-to-blade passage at its most efficient pump operation. The reduction of radial velocity can be found on the pressure surface. When the discharge is decreased with the guide vanes having the same opening, reverse flows are created at the leading edge of the runner. Efficiency and head suddenly changes, and vibration

Fig.7 Velocity and pressure distributions at the inlet in low discharge pumping operation

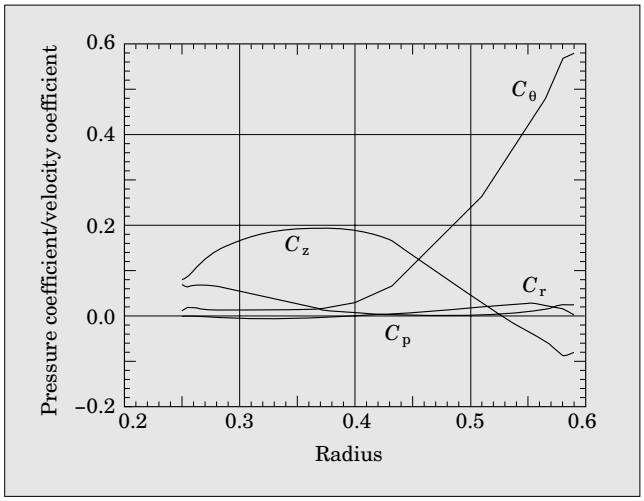

Fig.8 Velocity vectors at partial discharge

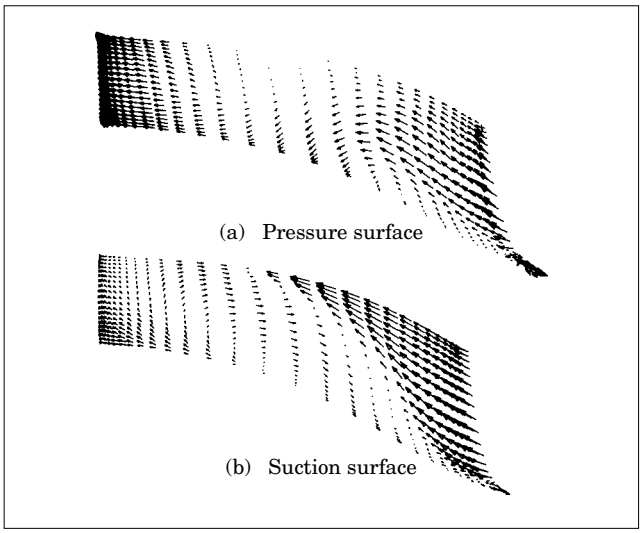

Fig.9 Computational results for the low-pressure range

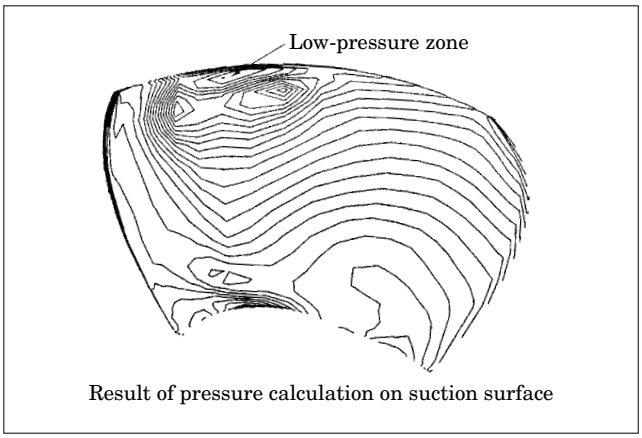

Fig.10 Erosion near the tip side on the suction surface of actual runner

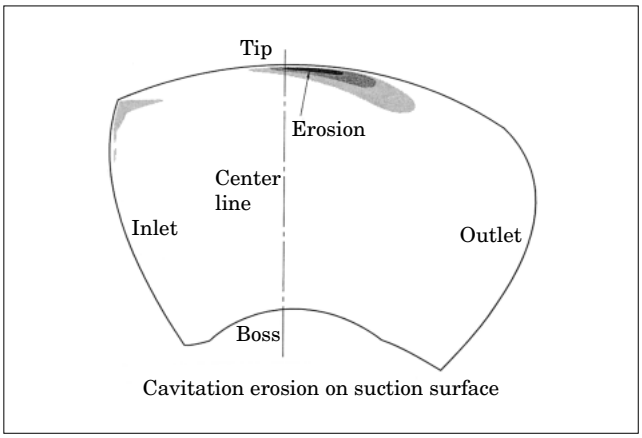

Fig.11 Tip leakage flow and vortex near tip side

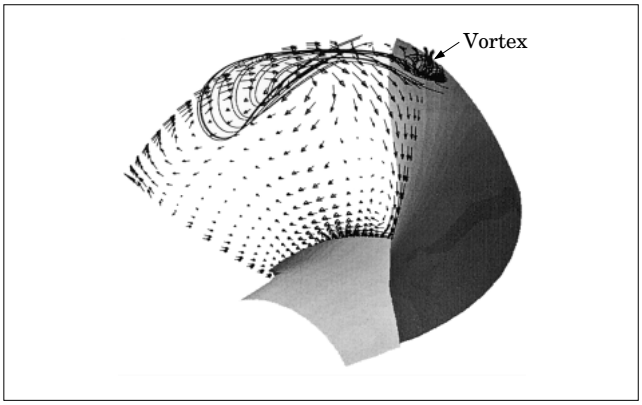

and noise occur at the partial discharge operating conditions. Figure 7 shows the velocity and pressure distributions of the pump inlet in the case of reverse flow generating at the leading edge. The abscissa is the radius, the left side is the crown, and the right side is the band. Axial velocity C_z starts decreasing from midspan toward the band side and is negative near the band side. It is understood that C_θ increases steeply in the same area. It is possible to say that reverse flow occurs at the band side in this operating condition when such results are analyzed. Figure 8 shows the velocity vectors on the pressure and suction surfaces at this operating condition. A strong reverse flow is observed near the band side. Moreover, this reverse flow area expands from the pressure side toward the suction side. It can be confirmed that efficiency and head decrease due to reverse flow[(3)].

The performance and appearance of the flow of the pump-turbine model in the initial design stage are obtained by computational results. From these results, the initial design can be evaluated, and any redesign for the next stage can be drawn. The accumulation of such analytical information and the improvement in both the analytical technologies and computational environments will contribute to building a more reliable tool for pump-turbine design.

2.3 Kaplan turbines

An existing Kaplan turbine runner to be replaced is also analyzed. The specific speed of this Kaplan turbine is n_{SQ} = 156 (r/min, m³/s, m) at the maximum efficiency point. As in bulb turbines, there exists the leakage flow through the gap along the blade outer periphery in Kaplan turbines. In high head machines, cavitation erosion can be generated due to this leakage. The Kaplan turbine mentioned in this paper was manufactured in the 1960's, with the discharge ring designed as a complete cylinder. Therefore, the gap expands at the leading and tailing edges by an increase in the runner opening. Figure 9 shows the pressure contours on the suction surface obtained by the analysis. A narrow, low-pressure area can be seen a little upstream of the runner's center line near the tip side, and a high-pressure range exists adjacent to this low-pressure range. Moreover, a low-pressure area is also found along the leading edge. In this turbine, extremely violent cavitation erosion was generated in the suction surface of the blade tip side, as shown in Fig. 10. In particular, the heaviest erosion occurs on the blade suction surface, where the gap is minimal in size. The dark color in this figure shows that erosion is heavy. Although the low-pressure range of the computational result appears a little upstream in comparison with the actual erosion, the shapes of the two results are very similar.

In Fig. 11, the flow field near the tip side on the suction surface is shown with the velocity vectors and streamlines. It is understood that a thin, strong tip vortex is formed near the center of the runner where the gap is narrow. Moreover, the high-pressure belt observed in Fig. 9 is dependent on stagnant pressure. This in turn is a blade-to-blade secondary flow that collides with the blade suction surface at the inside of the tip vortex.

3. Conclusion

The development of three-dimensional analysis technologies and the computational results of the hydraulic turbines and pump-turbines are introduced. More detailed information regarding flow through the hydraulic turbine and pump-turbine can be obtained now than in the past by the advancement of the three-dimensional flow analysis technology. It is expected to achieve a wide but steady operating range by improving the efficiency of hydraulic turbines and pump-turbines.

However, the CFD technologies which have been developed are not perfect and have limitations in the field of numerical techniques and turbulent models. When commercial software is used, there are many instances where the computational results greatly differ from the actual flow in the case of complicated flow. Great care must be taken to recognize these occurrences. Therefore, the designer must perform flow analysis after fully understanding the suitable range of application for the computational code and the turbulent model. The hydraulic turbine's internal flow is a compound flow, as explained above, with separation, cavitation, and a strong vortex. Selection of the best computational techniques is necessary, in accordance with the various types and operating conditions of the hydraulic turbine.

As a quantitative design tool, the improvement of analysis technologies and the improvement of analytical accuracy and reliability is an important topic for the future. The mission of the design tool is to point the way for design improvement by analyzing performance defects of the hydraulic turbine. We intend to advance both utility and analytical technologies aiming at the achievement of the higher level CFD technology, by which the design can be completed through "Numeric experimentation" without relying on the model test.

References:

(1) Y. Qian, et al: Numerical Flow Simulation on Channel Vortex in Francis Runner, XVII IAHR Symposium, Beijing, (1994)

(2) Y. Qian, et al: 3-D Numerical Analysis of Bulb Turbine Runner Performance with and without Tip Clearance, FED-Vol.227, Numerical Simulation in Turbomachinery ASME, (1995)

(3) Y. Qian, et al: Analysis of The Inlet Reverse Flows in a Pump Turbine using 3-D Viscous Numerical Techniques, XVIII IAHR, (1996)

Technologies to Modernize Existing Hydropower Plants

Takayuki Okuno
Yoshiaki Araki
Masaru Iijima

1. Introduction

Japan's hydropower plants occupy an important position as entirely domestic, clean energy sources and new development of hydropower plants is promoted to ensure a stable energy supply.

The history of hydropower plants in Japan is long (about 100 years) and Fuji Electric has supplied hydropower equipment for nearly 60 years. Deteriorated hydropower plants erected before the 1950s still remain in large numbers.

Formerly, these plants that have been in operation for a long time are restored to their initial condition mainly by repairing only severely deteriorated parts.

However, there is a demand for reducing the labor involved in maintenance and inspection due to the trend in unmanned hydropower plants. There are also demands for environmental protection measures to prevent pollution that are stricter than when the plants were originally built. Performance of the main unit sometimes has to be reconsidered in response to changes in the river flow and operating conditions. Also, the number of skilled engineers for maintenance is insufficient. Because of these changes in the environment around existing hydropower plants, customer needs for repair and modernization are diversified. Therefore, recent existing hydropower plants have undergone integrated modernization by incorporating measures for reduced labor, higher efficiency, environmental protection, improved performance of the main unit, equipment simplification, and improved reliability.

This paper, based on recent technical trends to meet current needs, introduces several characteristic examples of modernization technologies for the equipment.

2. Trend of Modernization Technologies

A summary of the technologies used for modernizing the equipment is shown in Table 1.

Amongst hydropower equipment, systems for cooling water and pressurized oil have the most complicated configuration and require the most labor for maintenance. Eliminating devices that use these systems will simplify the equipment and increase reliability. Therefore, in the modernization of equipment, the application of technology to omit pressurized oil, air, and cooling water, the so-called "three-less" technology, is the most important topic. Many new technologies aimed at a wide range of applications have been developed.

In consideration of the global movement for environmental protection which has become stricter, technologies to prevent oil leakage into rivers and to eliminate toxic materials are the main focus of modernization technologies.

With the goal to simplify equipment and provide advanced functions, application of digital technology to control equipment is increasing. The establishment of digital added value technologies such as automatic patrol inspection systems to improve maintenance efficiency will also be an important topic in the future to improve the management techniques of power generating systems.

Table 1 mainly describes new technologies used for equipment modernization. In the future, it is anticipated that there will be greater demands for enhanced technology to restore deteriorated equipment under the existing restrictions.

3. Modernization Technologies

3.1 Modernization Technologies for hydraulic turbines

3.1.1 Waterless cooling system

The water supply equipment at hydropower plants contains many components, malfunctions most frequently, and thus requires much labor to maintain.

Therefore, the elimination of this water supply equipment, known as waterless design, is a major theme in the modernization of hydropower equipment to reduce the incidence of malfunctions, simplify maintenance, and shorten inspection time.

(1) Use of air cooled oil-immersed turbine bearings

Many existing oil lubricated type hydraulic turbine-generators have used river water as the water for cooling.

Waterless cooling systems for turbine bearings

Table 1 Modernization technologies for hydropower equipment (summary)

User needs		Turbines	Generators	Control
Reduction of maintenance	Waterless cooling	• Waterless shaft seal • Air-cooled bearing	• Pipe-ventilated generators • Air-cooled bearing • Heat pipes	Digital solid-state circuits
	Oilless (greaseless)	• Motor-operated servomotor • Water-lubricated bearing • Oilless bearings	• Electromagnetic braking	
	Airless	• Elimination of air compressors (bladder type oil pressure device)	• Electromagnetic braking	
	Oil mist prevention		• Shaft seal device with magnetic fluid	
	Extended life span, etc.	• Wear resistant material to prevent cavitation (utilizing ceramic technology) • Solid-state sensors	• Brushless exciters • Solid-state sensors	
Environmental protection	Prevention of oil leakage into rivers	• Kaplan runner boss immersed in water • Water-lubricated bearing • Oilless bearings		
	Elimination of pollutants		• Non-asbestos brake lining	
Economical improvement	Increase in annual power output	• Turbine runner efficiency improvement		Expansion of total digital control systems
	Reduction of size and weight	• High specific speed runners • Runaway speed machine (reduction of guide vane closing speed, increase of ΔN by omitting the pressure regulator)	• Runaway speed machine (runaway speed machine design with specific generator GD^2)	
	Equipment simplification	• Elimination of the spillway (deflector discharge, etc.) • "Three-less" devices (waterless, oilless & airless)	• "Three-less" devices (waterless, oilless & airless)	
Management technique improvement	Preventive maintenance	• Life expectancy diagnosis	• Life expectancy diagnosis	Preventive maintenance and automatic patrol inspection
	Condition monitoring	• Condition monitoring sensor technologies	• Condition monitoring sensor technologies	
Advanced functions				Expansion of total digital control systems

Table 2 Record of air-cooled vertical hydraulic turbine bearings

User	Plant name	Turbine type	Output (kW)	Speed (r/min)	Cooling	Start date	Remarks
Nipponkai P. Gen. Inc.	Katagai Minamimata	VP	5,230	450	Fan cooler	Oct. 1989	New machine
Tohoku E. P. Co. Inc.	Ohzaso	VP	12,000	375	Fan cooler	Apr. 1991	New machine
Chubu E. P. Co. Inc.	Shichiso	VF	2,380	200	Air cooling	May 1991	New machine refurbished
Chugoku E. P. Co. Inc.	Shibakigawa No. 2	VF	6,900	450	Air cooling	Mar. 1992	Existing, modified
Hokkaido E. P. Co. Inc.	Shikaribetsu No. 2	VF	7,700	500	Air cooling	Aug. 1994	Existing, modified
Tohoku E. P. Co. Inc.	Gassan	VD	9,160	500	Fan cooler	Under development	New machine

Note (1) "Air cooling" in the Cooling column indicates a naturally cooled air cooling system.
(2) "Fan cooler" in the Cooling column indicates a separately installed fan-cooled oil cooler system.

Fig.1 Outline of the mechanical seal

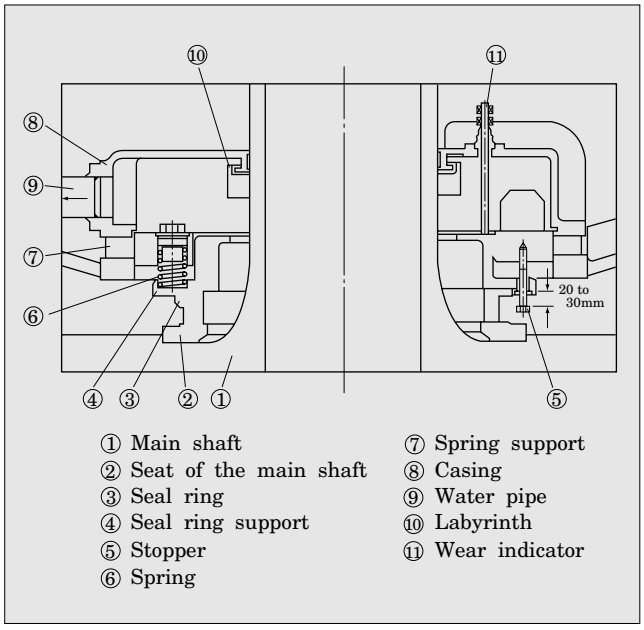

include natural air cooling, fan cooling with a separate oil-to-air heat exchanger, heat pipe cooling for horizontal machines, etc.

The application of heat pipe cooling is limited to low power horizontal-shaft machines because of the characteristics of the working medium. Natural air cooling and fan cooling systems can be applied to vertical-shaft machines. The range of these applications has been widened recently.

The natural air cooling system cools the lubricant by heat radiation from the external surface of the

bearing oil tank and is an ideal system that needs no extra attachments such as a power source. Recently, this system has expanded its application range while accumulating the following features.

(a) Fins are attached to the external wall of the oil tank to raise heat radiation efficiency.
(b) Heat radiation is similarly improved by widening the effective heat radiation area as well as securing space around the oil tank.
(c) A low viscosity lubricant, VG46, is used to reduce heat generation in the bearings.
(d) Use of segment type bearings reduces heat generation.
(e) The guaranteed maximum bearing temperature is raised from 65°C (former value) to 75°C.

On the other hand, the fan cooling system cools heated lubricant by drawing it into an air-cooled oil cooler equipped with an electric fan. This system has a wider application range than the natural air cooling system as long as space to install the oil cooler with fan can be secured.

Table 2 shows application examples of these air cooling systems.

(2) Shaft seal device using ceramics

In conventional shaft seal devices, gland packing and carbon packing were widely used. These both required complex water supply devices to remove dust and sand from the supply water. Other disadvantages were that repeated tightening was necessary for gland packing and carbon packing would rapidly wear in a short time once abnormal wear occurred. The development of a shaft seal device which needs no clean water supply, has higher reliability, and a long life span, is hoped for.

Application of the labyrinth seal with no sliding parts is worth investigating first. However, its application is limited to use with low tail water levels, and is therefore seldom used.

Recently, Fuji Electric has developed a mechanical seal type shaft seal device which uses a ceramic compound material for the sliding surface and a special synthetic resin for the seal material. This seal device was applied to a certain existing hydraulic turbine and was successful in yielding a low wear rate and stable performance. Figure 1 is an outline of this device. Instead of a clean water supply, the mechanical seal type only requires a small quantity of river water at atmospheric pressure for cooling.

Fuji Electric is now promoting studies on the combination of ceramic materials.

3.1.2 Oilless (greaseless) Technologies

(1) Water-lubricated bearings

Previously, grease-lubricated bearings were generally used in Kaplan turbines. However, grease-lubricated bearings required a constant supply of grease for lubrication. Once used, the grease would flow out into the river. Recently to prevent pollution, there has been a growing demand for greaseless bearings and a water-lubricated bearing was developed as a replacement.

Figure 2 shows an example of a water-lubricated bearing structure.

The water-lubricated bearing uses water for the lubricant and glass fiber reinforced phenol resin wound in layers for the bearing surface material. Fuji Electric uses a hydrodynamic lubrication system. The hydrodynamic lubrication system efficiently uses the shaft rotation and water viscosity to form a wedge-shaped water film between the shaft and bearing and supports the bearing load with this water film. Therefore, as this system does not require a pressurized water supply at the bearing surface (as used for hydrostatic bearings) it has the special feature of being a self-contained system.

Since unit No. 1 started operation in 1984, the number of Fuji Electric's applications of this bearing system amounts to 15 existing modernized turbines and to 20 when new turbines are included, all of which continue satisfactory operation.

(2) Application of the motor-operated servomotor

In conventional hydropower plants, guide vanes, inlet valves, and pressure regulators were generally operated by oil pressure. However, oil pressure devices consist of pipes, valves, and many other components, and as a result are prone to oil leakage. Various parts will be contaminated by an oil leak, and there is also the danger of fire in case pressurized oil is sprayed. For these reasons, this device was difficult to maintain.

In consideration of these problems, if the guide vane mechanism is made to operate electrically and the oil pressure device is omitted, the station equipment will be much simplified, and the amount of equipment to maintain as well as the required labor will be greatly reduced.

In addition, the electrical operation of guide vanes makes it possible to eliminate pressure regulators in stations such equipped.

In this case, to limit the water pressure rise in the penstock generated by the sudden closing of the guide vanes to values as in conventional devices, it is necessary to close the guide vanes slowly. Accordingly, the hydraulic turbine generator shall tolerate a speed rise at load rejection up to the runaway speed of the prime mover, a so-called runaway speed machine.

However, the fatigue strength of the rotor components becomes a problem for the generator.

As long as steel plates produced under the present manufacturing technology and high quality control are used, fatigue strength is not a big problem. However, because most of the machines currently being refurbished were manufactured during the postwar rehabilitation period and are subject to repeated stress, it is difficult to ensure their continuous use. Therefore it is necessary to replace the main rotor parts in these machines.

Fig.2 Example of a water-lubricated bearing structure

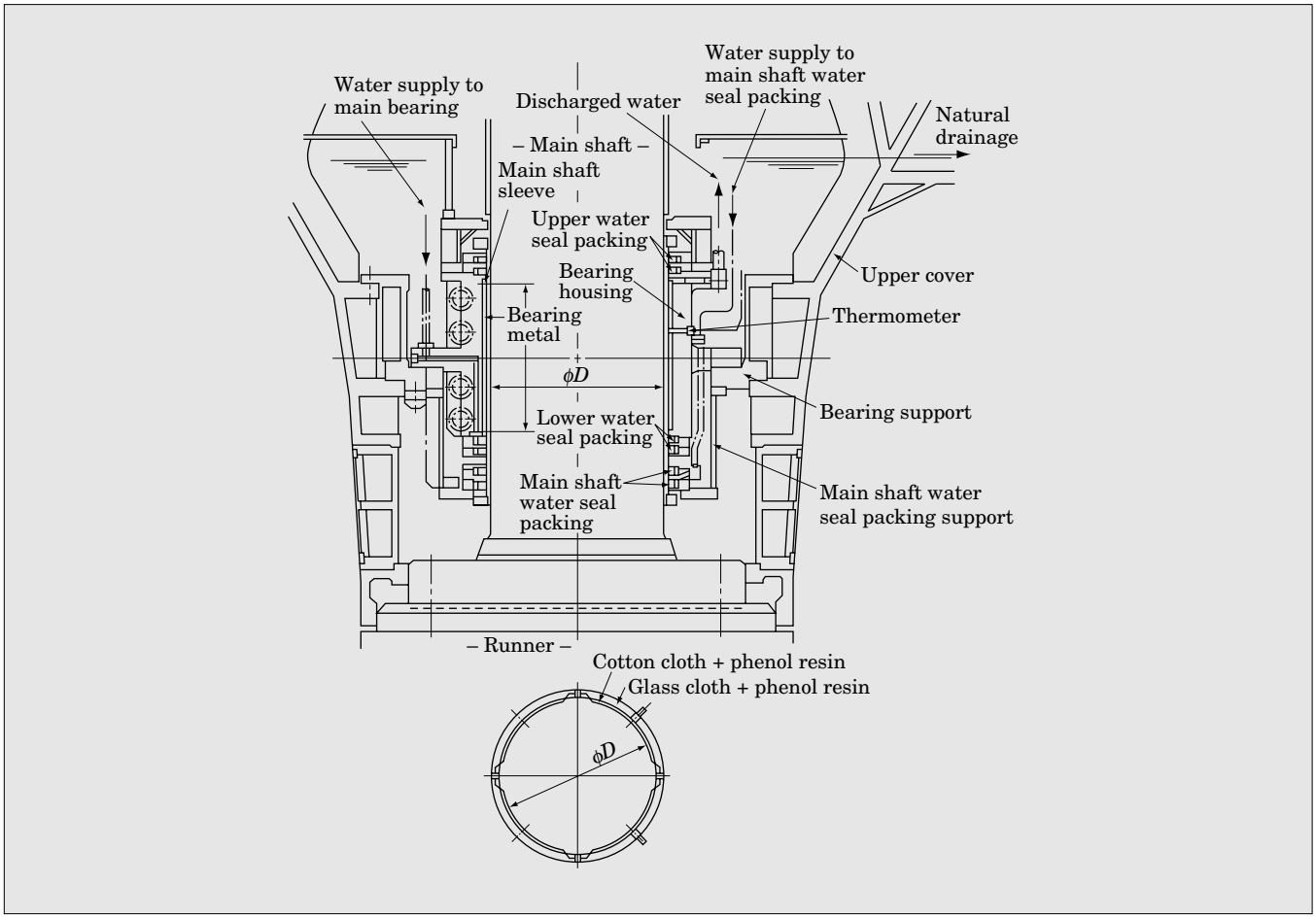

Fig.3 Elements of a motor-driven servomotor system

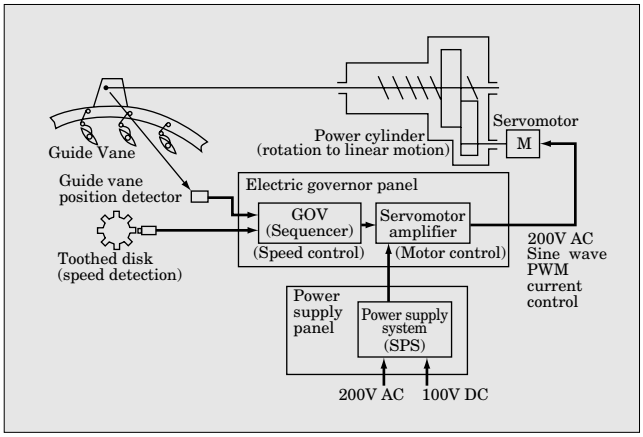

Fuji Electric's motor-operated servomotors have been used in applications since 1978. Currently 86 units are in operation, including new installations. Figure 3 is a diagram to show the elements of a motorized power cylinder which converts the motor's rotational motion into linear motion of the output shaft.

Fuji Electric formerly used a DC brushless system, but with the improvement of inverter technology, has utilized an AC brushless system in applications with a larger output. At present, an AC vector control system is applied to rated outputs of 22kW or more.

The applicable range of motor-operated servomotors is not more than 20,000 kW for generator output, 30 kW for motor output, and 295 kN for rated thrust.

In the repair of existing machines, however, sometimes the installation of a motor-operated servomotor is restricted by space and each case must be considered individually.

Motor-operated servomotors have already been applied not only to Frencis turbines but also to operate Pelton turbine needles and deflectors. Application to the operation of Kaplan turbine runner vanes is now under development.

3.2 Modernization technologies for generators

3.2.1 Shaft seal device with magnetic fluid

Fuji Electric prevents oil vapor leakage from the shaft seal of the bearing oil tank by partitioning the inside and outside of the oil tank with an air curtain using the labyrinth system shown in Fig. 4 as a standard structure.

However, because the relation between pressure inside and outside of the oil tank and air pressure sealed in the labyrinth part can not be ideally regulated, it is difficult to stop leakage completely.

Fig.4 Labyrinth type shaft seal device

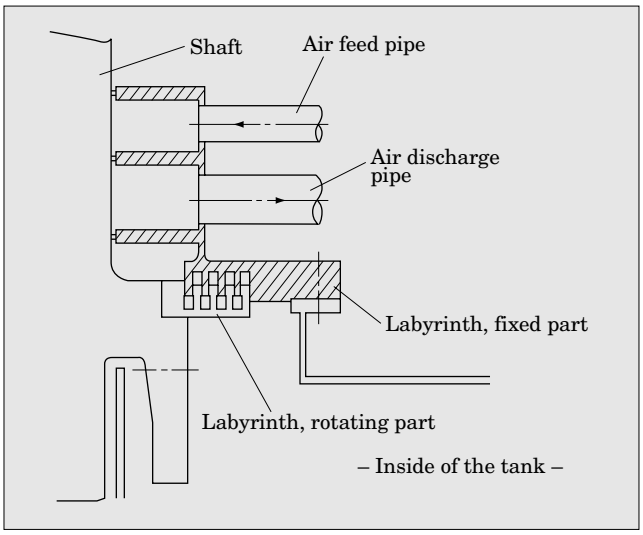

Fig.5 Shaft seal device using magnetic fluid

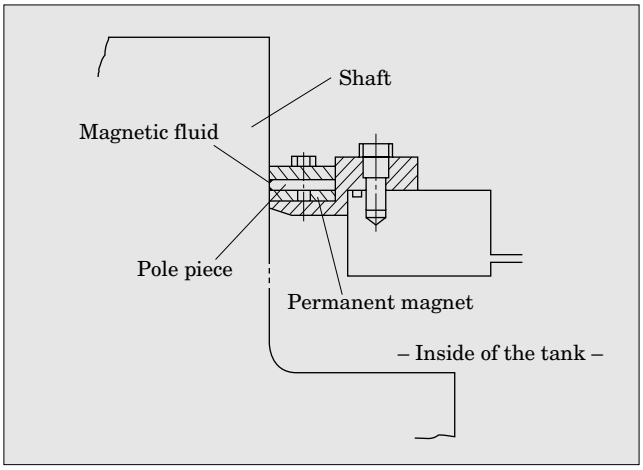

Before hydropower plants were unmanned, it was thought that oil leakage from the bearings was unavoidable and would be monitored by the maintenance staff, oil leaks were unimportant as long as there was no undesirable effect. Now in unmanned plants, even stains due to oil vapor are considered a problem.

Until now, all of the types of shaft seals have had a clearance between the shaft and oil mist cover.

The shaft seal device introduced here, as shown in Fig. 5, completely fills this clearance with magnetic fluid to stop oil vapor leakage.

The permanent magnet mounted on the inside of the oil mist cover forms a magnetic circuit through the clearance between the shaft and oil mist cover. The magnetic force holds the magnetic fluid in its position.

However, for high shaft peripheral speeds, there is a problem in that the magnetic fluid is vaporized by frictional heat or scattered by centrifugal force. Therefore, this device can not be applied to all machines.

Currently, one such device is being manufactured for application in a specific plant. It is desired to use this device in applicable machines in the future in order to reduce maintenance labor.

Fig.6 Air flow when one unit is in operation

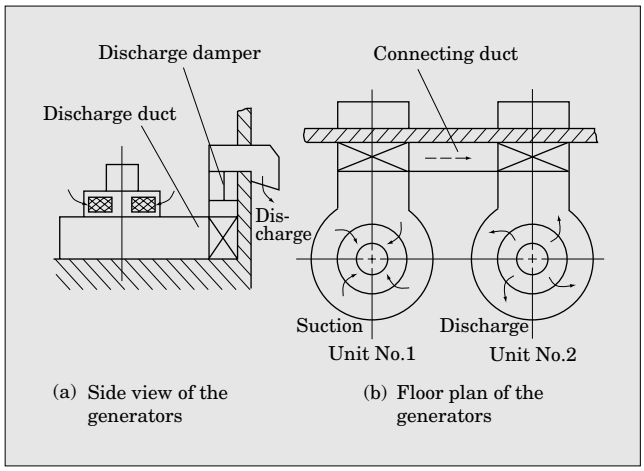

3.2.2 Measure to maintain insulation resistance

In hydropower plants in which more than one pipe-ventilated generator is installed, the insulation resistance of the generator not in operation greatly drops and when started, the field winding ground detector relay may activate.

The reason for this behavior is that the generator in service takes in the room air and discharges it outdoors. Simultaneously, the same quantity of outside air is drawn into the generator room through the fresh air inlet. Because the building fresh air inlet is usually equipped with dust and insect filters, pressure inside the building is made a little negative by the flow resistance. As a result, the outside air flows backward from the exhaust port of the generator not in operation, and flows around the field windings and armature windings into the generator room.

Therefore, when humidity is high, the windings are directly exposed to moist outside air, and the deteriorated, absorbent insulation cannot maintain the appropriate insulation resistance, resulting in activation of the field winding ground detector relay. As a measure to prevent insulation resistance from dropping, a space heater is provided, but this is not effective when exposed to the flow of outside air.

This problem has been solved by connecting the discharge ducts of several generators, providing motor-operated discharge dampers, and attaching opening regulators. Using Fig. 6, these measures are introduced below.

When both units No. 1 and No. 2 are in operation, air does not flow in the connecting duct. When unit No. 2 stops, part of the discharge of unit No. 1 flows in the connecting duct. By closing the discharge damper, that discharge is returned through the No. 2 generator to the generator room.

As a result, although pressure inside the plant is negative, the discharge of unit No. 2 does not have negative pressure and therefore does not such in outside air. Moreover, since the unit is filled with air

heated by unit No. 1, having low relative humidity, the insulating material absorbs no moisture and the insulation resistance can maintain the appropriate value. In addition, the amount of flow backward into the room is related to the room temperature, and a rise in room temperature raises the winding temperature. Therefore, by changing the opening of unit No. 1's discharge damper, the discharge quantity and flow backward can be regulated to keep the room temperature at a prescribed value. Further, in winter when one unit is operated for a long period of time, not only can this system maintain the insulation resistance, but can also heat the room air and solve the problem of frozen plant equipment.

4. Conclusion

This paper introduces several characteristic examples of recent modernization technologies that Fuji Electric is developing for existing hydropower plants.

In the future, customer needs for refurbishing existing hydropower equipment will become more and more diversified. It is hoped that the reader finds this paper helpful in repairing deteriorated equipment.

Global Network

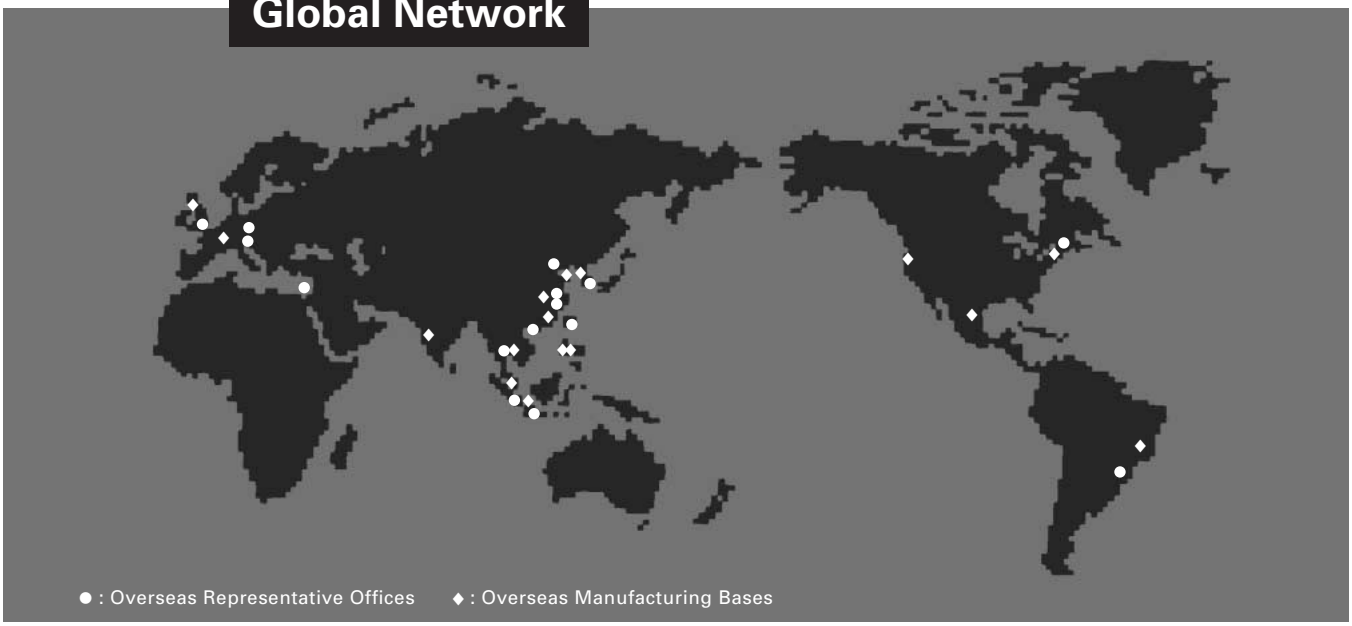

AMERICA

■FUJI ELECTRIC CORP. OF AMERICA
●Head Office
Park 80 West Plaza Ⅱ, Saddle Brook, NJ07663, U.S.A.
TEL : (201) 712-0555 FAX : (201) 368-8258

■FUJI ELECTRIC DO BRASIL INDUSTRIA E COMERCIO LTDA.
Rua Guajajaras, 1707, Barro Preto,
CEP 30180-101 Belo Horizonte, M. G., BRASIL
TEL : (031) 291-5161 FAX : (031) 291-8185

EU

■FUJI ELECTRIC CO., LTD.
Erlangen Representative Office, Sieboldstr. 3, D-91052
Erlangen, F.R. GERMANY
TEL : (09131) 729613, 729630 FAX : (09131) 28831

■FUJI ELECTRIC GmbH
Lyoner Str. 26,
D-60528 Frankfurt am Main, F.R. GERMANY
TEL : (069) 6690290 FAX : (069) 6661020

■FUJI ELECTRIC CO., LTD.
London Representative Office, 40 George Street,
London W1H 5RE, U.K.
TEL : (0171) 935-0544 FAX : (0171) 935-6893

■FUJI ELECTRIC (U.K.) LTD.
40 George Street, London W1H 5RE, U.K.
TEL : (0171) 935-0544 FAX : (0171) 935-6893

ASIA

■FUJI ELECTRIC CO., LTD.
Beijing Representative Office, Suite 3603, China World Tower,
China World Trade Center No. 1, Jian Guo Men Wai Avenue,
Beijing 100004, THE PEOPLE'S REPUBLIC OF CHINA
TEL : (010) 6505-1263, 1264 FAX : (010) 6505-1851

■FUJI ELECTRIC CO., LTD.
Hangzhou Representative Office, #402 Heng He Bldg.,
23-2 Huan Cheng Dong Lu Hangzhou City, Zhejiang Province,
THE PEOPLE'S REPUBLIC OF CHINA
TEL : (0571) 704-5454 FAX : (0571) 704-3089

■SUZHOU LANLIAN-FUJI INSTRUMENTS CO., LTD.
Songlin Economic & Technical Development
Zone, Wujiang City, Jiangsu Province 215200,
THE PEOPLE'S REPUBLIC OF CHINA
TEL : (05223) 41-1594 FAX : (05223) 41-1654

■FUJI ELECTRIC TECHNOLOGY AND SERVICE (SHENZHEN) CO., LTD.
No. 44 Dongjiao Street., Zhongxing Rd., Shenzhen City,
Guangdong Province 518014,
THE PEOPLE'S REPUBLIC OF CHINA
TEL : (0755) 220-2745 FAX : (0755) 220-2745

■FUJI ELECTRIC CO., LTD.
Taipei Representative Office, 5th Fl.,
Taiwan Fertilizer Bldg., No. 90, Nanking E Rd.,
Sec.2 Taipei, TAIWAN
TEL : (02) 561-1255, 1256 FAX : (02) 561-0528

■FUJI/GE (TAIWAN) CO., LTD.
12F, No.70, Cheng Teh N. Rd., Sec.1, Taipei, TAIWAN
TEL : (02) 556-0716, 9061 FAX : (02) 556-0717

■FUJI ELECTRIC (ASIA) CO., LTD.
10th Fl., West Wing Tsimshatsui Centre, 66 Mody Rd.,
Tsimshatsui East Kowloon, HONG KONG
TEL : 2311-8282 FAX : 2312-0566

■FUJI ELECTRIC KOREA CO., LTD.
16th Fl. Shinsong Bldg. 25-4 Youido-Dong,
Youngdungpo-Gu, Seoul, 150-010, KOREA
TEL : (02)780-5011 FAX : (02)783-1707

■FUJI ELECTRIC CO., LTD.
Bangkok Representative Office, Room No.1202, 12th Fl.
Two Pacific Place
142 Sukhumvit Rd. Bangkok 10110, THAILAND
TEL : (02) 653-2020, 2021 FAX : (02) 653-2022

■P. T. BUKAKA FUJI ELECTRIC
Plaza Bapindo, Menara Ⅰ, 24th Fl. Jl. Jendral Sudirman Kav,
54-55 Jakarta 12190, INDONESIA
TEL : (021) 5266716～7 FAX : (021) 5266718

■FUJI ELECTRIC CO., LTD.
Singapore Representative Office, 401 Commonwealth Drive,
#04-05 Hawpar Technocentre, Singapore 749598, SINGAPORE
TEL : 479-5531 FAX : 479-5210

■FUJI ELECTRIC SINGAPORE PRIVATE LTD.
401 Commonwealth Drive, #04-05 Hawpar Technocentre,
Singapore 749598, SINGAPORE
TEL : 479-5531 FAX : 479-5210

■FUJI/GE PRIVATE LTD.
171, Chin Swee Rd., #12-01/04 San Center,
Singapore 169877, SINGAPORE
TEL : 533-0010 FAX : 533-0021

■HOEI ELECTRONICS (S) PRIVATE LTD.
51 Goldhill Plaza, #14-09/10 Newton Rd.,
Singapore 368025, SINGAPORE
TEL : 251-8751 FAX : 251-0827

■GE/FUJI ELECTRIC CO., LTD.
Nicolaou Pentadromos Centre, Office 908,
Block A, P. O. Box 123, Limassol 205, CYPRUS
TEL : 5-362580 FAX : 5-365174

Fuji Electric, the Pioneer in Energy and Electronics

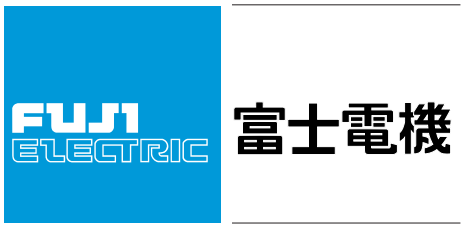

Printed on recycled paper